

The Dynamics and Energetics of Mature Tropical Cyclones

RICHARD A. ANTHES

*Department of Meteorology, Pennsylvania State University
University Park, Pennsylvania 16802*

Rapid progress toward the understanding of tropical cyclones has been made during the past 10 years, largely as a result of the development of numerical models. The dynamics and energetics of the mature tropical cyclone are reviewed in this article. First, the pressure, wind, temperature, and moisture structures of the hurricane are summarized. Then a scale analysis is applied over four separate regions of the hurricane domain to emphasize the most important dynamic processes in each region. The energetics of the tropical cyclone is examined in detail. The storm is shown to be a self-sustaining quasi-steady thermodynamic heat engine that is driven primarily by latent heat release. The relationship between latent heating and production of kinetic energy is discussed from the available potential energy viewpoint. The possibility of a steady state axisymmetric hurricane in a closed domain is considered. Although such a model appears possible from an energetic viewpoint, angular momentum considerations reveal that a steady axisymmetric closed system is impossible on any scale. For small domains (radius ~ 500 km), in which axisymmetric circulations are possible, the system must be open in order that angular momentum be imported from the environment. For larger domains, axisymmetric circulations are unrealistic. The water vapor budget of the hurricane is examined to indicate the relative importance of evaporation and horizontal transport of water vapor in maintaining the moisture supply. Evaporation is shown to be an important percentage of the precipitation in the mature storm. Finally, the numerical modeling of tropical cyclones is summarized. An important problem in the development of hurricane models is the treatment or parameterization of the cumulus cloud scale and the hurricane scale interactions. The implications of the concept of conditional instability of the second kind on hurricane modeling are discussed. Results from several axisymmetric (two-dimensional) hurricane models, including attempts to simulate hurricane modification experiments, are summarized. Some recent results from a time-dependent three-dimensional hurricane model are presented.

CONTENTS

Structure of the mature tropical cyclone	496
The hurricane eye	496
Surface pressure	497
Temperature structure	497
Wind structure	497
Moisture and precipitation distribution	497
Dynamics of the tropical cyclone	499
Horizontal and vertical diffusion of momentum	501
Scale analysis of horizontal equations of motion	503
Dynamics of the hurricane eye	505
Scale analysis of thermodynamic equation	506
Energetics of the tropical cyclone	507
Kinetic energy budget	507
Available potential energy budget	508
Angular momentum considerations in the tropical cyclone	510
Development of angular momentum budget equations	511
Angular momentum distribution in the hurricane	512
Water vapor budget of the tropical cyclone	513
Water vapor budget equations	513
Empirical water vapor budgets	515
Modeling of tropical cyclones	515
Carrier's steady state hurricane model	516
Prognostic models	517
A three-dimensional hurricane model	519
Summary of model results	519

A. INTRODUCTION

The mature tropical cyclone has always been a fascinating atmospheric disturbance, mainly because of the catastrophic effect these small but intense storms occasionally wreak on human activities. The hurricane is the most destructive of all natural disasters; for example, over 17,000 lives have been lost in the United States alone since 1900 owing to hurricanes, and it is estimated that the economic loss in the United States exceeds \$100 million annually [Dunn and Miller, 1964]. In addition

to the interest generated by its awesome powers, the hurricane is a distinct isolated atmospheric phenomenon that only occasionally disturbs the tropical peace and as such is an appealing object for meteorological investigation. The effect of numerous empirical and theoretical studies during the past 25 years has been tremendous progress in understanding these destructive but intriguing storms. This article reviews present knowledge about the dynamic and energetic balances involved in the maintenance of hurricanes and summarizes recent advances in the modeling of these storms.

A tropical cyclone is defined as a warm core cyclonic wind circulation in which the maximum sustained wind is 35 knots (40 mi/h) or greater. Tropical storms in which the maximum wind equals or exceeds 65 knots (74 mi/h) are called hurricanes when they occur in the Atlantic and typhoons in the Pacific.

The horizontal scale of the typical hurricane circulation may be defined by the radius of the subnormal surface pressure anomaly, about 1000 km, although the size of the individual storms may vary within a factor of 2 of this figure. The average radial extent of hurricane force winds is only about 100 km, but gale-force winds (winds greater than 28 knots) may extend 500 km from the center [Dunn and Miller, 1964]. The diameter of the storm's cirrus cloud shield, which is produced by the intense upward vertical motion near the center and is then advected outward by the upper-level winds, is typically 600–800 km.

The hurricane circulation extends throughout the entire troposphere. The intensity of the circulation is strongest in the lower troposphere and weakens gradually with increasing height. The stratosphere is relatively undisturbed; therefore the vertical scale of the hurricane may be defined by the tropopause height of about 15 km.

Intense rainfall occurs in the rising air near the center of hurricanes; for example, Silver Hill, Jamaica, reported an extreme figure of 245 cm of rain associated with a hurricane passage in 1909 [Dunn and Miller, 1964]. Thus it has been realized for some time [Espy, 1841] that the latent heat of vaporization associated with the heavy rainfall is an important energy source for the tropical storm. Tropical cyclones form over tropical oceans that exceed 26°C in sea surface temperature [Palmén, 1948], and they occur most frequently during the warmest 4 months of the year. Their formation is favored in regions in which large cyclonic relative vorticity exists in the lower troposphere and the vertical wind shear is weak. A favorable position for these two conditions is the poleward side of the equatorial trough, where large-scale cyclonic horizontal shear is present. Eighty-seven percent of all storms form poleward of 20° latitude [Gray, 1967b], the indication being that the local vertical component of the earth's rotation plays a significant role in their development. Seventy-five percent of all tropical storms develop in the northern hemisphere, the Pacific Ocean spawning over 50% of the global total [Gray, 1967b]. Tropical storm formation usually proceeds from a preexisting tropical disturbance that consists of organized cloud and wind patterns. However, only about 10% of all tropical disturbances reach storm intensity, in spite of the superficially similar synoptic conditions associated with each disturbance. Thus the forecaster has the extremely difficult problem of somehow detecting in advance which disturbances will develop [Simpson *et al.*, 1968].

The average life-span of hurricanes is of the order of 1 week, but individual storms may survive indefinitely (greater than 4 weeks) if they remain over warm tropical water. The primary reason for the short average life expectancy is the tendency for tropical storms to move with the large-scale circulation out of the warm moist tropics where they originate and into the cooler more hostile environment of the middle latitudes.

In this review of the mature tropical cyclone we first summarize the three-dimensional pressure, temperature, wind, and moisture structure of the hurricane. These observational results form the basis for a scale analysis of the dynamic and thermodynamic equations that are relevant to the hurricane. The scale analysis shows that distinct regions of the tropical cyclone domain exist in which different physical processes are important.

Most of the tropical cyclone circulation is in gradient balance, the centripetal and Coriolis forces opposing the pressure gradient force. However, in the lowest kilometer or two, surface friction destroys the gradient wind balance, and air spirals inward toward the storm center, gaining kinetic energy as it accelerates toward low pressure. The strong cyclonic tangential circulation is produced by the inward advection of air with large absolute angular momentum from the hurricane environment. The inflowing air may not penetrate beyond some small radius, however, because of the excessively high velocities demanded by the quasi-conservation of angular momentum. Instead the air turns upward in the eye wall, an intense ring of cumulus convection surrounding the relatively calm clear eye.

When the air reaches the upper troposphere, the increased static stability forces it to turn outward, where it acquires an anticyclonic circulation relative to the earth. This anticyclonic circulation is a result of the loss of angular momentum to the sea along the air's low-level inflow trajectory. The outflow layer is quite asymmetric, and barotropic processes

appear to play an important role in maintaining the kinetic energy of the eddies.

After summarizing the important dynamic and thermodynamic processes in the hurricane circulation the energetics of the tropical cyclone is examined. The storm is shown to be a quasi-steady thermodynamic heat engine that is driven primarily by latent heat release. The link between latent heating and kinetic energy production is examined from the available potential energy viewpoint. The release of latent heat in the warm core maintains the hurricane's baroclinic structure and generates available energy, which is continuously converted to kinetic energy.

The energetics of the tropical cyclone suggests the possibility of modeling hurricanes with a steady state closed thermodynamic system with a horizontal scale on the order of several thousand kilometers. However, angular momentum considerations reveal that a steady axisymmetric closed storm domain on this scale is impossible. Instead large-scale eddies transport angular momentum from the environment into the storm system.

The water vapor budget also imposes constraints on the hurricane system and yields information on the role of evaporation and horizontal transport of water vapor in providing the moisture supply that is necessary for hurricane maintenance. An estimate of the depletion rate of preexisting water vapor in a system without evaporation is made. The ratio of evaporation to precipitation that is necessary to maintain a steady state moisture content in a domain with no net horizontal inflow of moisture across the outer lateral boundaries is also estimated.

Finally, the numerical modeling of tropical cyclones is reviewed. A major factor responsible for the progress in numerical modeling has been the differentiation between the cumulus cloud scale instability and the larger-scale instability associated with the development of the tropical cyclone (conditional instability of the second kind [Charney and Eliassen, 1964; Ooyama, 1964]). This second instability and the implications on hurricane modeling are discussed.

The analytic axisymmetric (two-dimensional) model of Carrier *et al.* [1971] is contrasted with several axisymmetric numerical models. Results from recent experiments with an asymmetric (three-dimensional) hurricane model are summarized.

B. STRUCTURE OF THE MATURE TROPICAL CYCLONE

Aircraft observations and satellite photographs have provided a reasonably complete picture of the three-dimensional structure of tropical cyclones. Although variations exist between individual storms, the characteristics discussed in the following subsections are typical and are present to an important degree in all tropical cyclones.

1. The Hurricane Eye

One of the most unusual and distinctive features of the mature hurricane is the eye, a more or less circular central region of the storm with a diameter varying between 5 and 50 km [Dunn and Miller, 1964]. The surface pressure attains its minimum value in the eye. The winds are light and variable inside the eye, in sharp contrast to the maximum winds that occur in the eye wall. The eye is typically free of significant cloud cover, in comparison to the surrounding region of thick clouds and torrential rainfall.

As was shown by Haurwitz [1935], subsidence of upper tropospheric air of high potential temperature is necessary to

achieve the extremely low hydrostatic surface pressure in the eye. The existence of this central core of subsidence is supported by the high temperatures [Sheets, 1969] and the absence of clouds. The dynamics of the eye and eye wall region are discussed in section C3.

2. Surface Pressure

The surface pressure field is one of the best known aspects of the hurricane. The surface isobars are nearly concentric circles with origin at the center of the storm. The minimum central pressure ever recorded is 887 mbar (about 90% normal atmospheric pressure), but a more common value is 950 mbar [Dunn and Miller, 1964]. Figure 1 shows the normalized surface pressure as a function of normalized radial distance, r/R_0 for the typical hurricane [Fletcher, 1955]. The notation is defined on page 520. The radial pressure profile closely follows the exponential function $P_n \approx \exp(-R_0/r)$ over the interval $0 \leq r_0/R_0 \leq 10$ [Meyers, 1957]; the pressure falls slowly in the outer region of the storm but drops sharply inside the 100-km radius. About 50% of the total pressure drop occurs within 80 km, which is about twice the radius of maximum wind.

3. Temperature Structure

One of the essential characteristics of the tropical cyclone is the warm central core. Temperature excesses on isobaric surfaces over the surrounding tropical environment are greatest in the upper troposphere, normally exceeding 10°C at the 10-km level. A cross section of potential temperature

$$\theta = T(P_0/p)^{\kappa} \tag{1}$$

through a mature hurricane (Hurricane Hilda, 1964) is shown in Figure 2. The horizontal temperature gradient beyond the 100-km radius is relatively weak, averaging about 0.5°C/100 km. Inside 100 km the temperature rises sharply and reaches a maximum inside the eye. In the lower troposphere the warm core exists only in the eye, and there is some evidence of a slightly cooler annular region surrounding the eye in the low levels. The radial temperature gradient in the lowest 1-km layer is comparatively small, a characteristic with important implications for the air-sea interactions to be discussed in a later section. Like the surface pressure field the temperature structure is quite symmetric about the storm center.

4. Wind Structure

Strong cyclonic flow dominates the hurricane circulation throughout most of the radial and vertical extent of the storm.

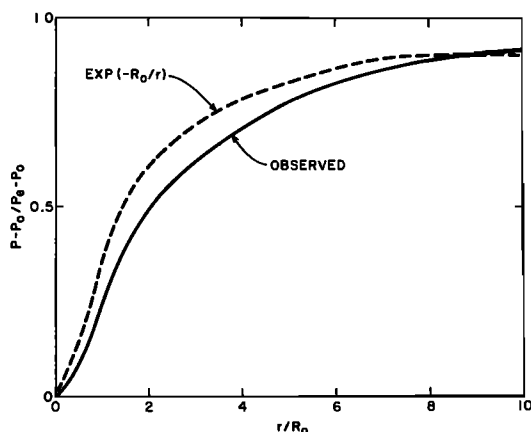


Fig. 1. Normalized surface pressure (P_n) as a function of normalized radius (r/R_0) for mature hurricanes [Fletcher, 1955].

Radial motion is confined to the lowest one or two kilometers (the inflow layer) and the upper few kilometers (the outflow layer). The lowest layer is the frictional (Ekman) boundary layer, in which turbulent eddies transport momentum and kinetic energy to the surface, where they are lost to the sea. Figure 3 shows a low-level radial profile of the wind speed for Hurricane Helene [Schauss, 1962]. In this storm, gale-force winds extend to 400 km. The wind crosses the circular isobars at an angle of 20–40° in this layer [Schauss, 1962], so that the radial component of the flow is a significant fraction of the tangential component. In many storms the low-level wind is approximately symmetric about the axis of rotation, at least within 300 km of the center. The radial variation is given frequently by the empirical law

$$V(r) = V(R_0)(R_0/r)^x \quad R_0 \leq r \leq r_0 \tag{2}$$

where x ranges from 0.5 to 1.0. This decay function is satisfied approximately only over moderate radial distance (~400 km); it is usually impossible to find one value of x that applies over the entire radial extent of the storm. The maximum wind $V(R_0)$ is typically 50 m s⁻¹ but may exceed 100 m s⁻¹ in extreme cases.

From the top of the boundary layer to a height of about 10 km the radial flow is negligible in comparison to the tangential flow, which decreases slowly in speed with height. From 10 km to the tropopause (~15 km) the hurricane circulation becomes quite asymmetric. This loss of symmetry is related to the greatly diminished radial pressure gradient, which is a hydrostatic consequence of the warm core system. The outflow occurs in one or two anticyclonically curving jets. These jets increase in scale with increasing distance from the storm center and eventually merge with the synoptic scale circulation. For example, the outflow layer for the intense Hurricane Camille (Figure 4) exhibits strong outflow mainly in the northeast and southeast quadrants.

The mean vertical motion throughout most of the hurricane circulation is weak. Subsidence occurs over a large area surrounding the storm (at radial distances greater than 300 km), as is evidenced by the nearly cloud-free atmosphere beyond this radius. (See Figure 5.) Diagnostic studies utilizing observations [Malkus and Riehl, 1960] and theoretical models [Rosenthal, 1970b] indicate typical midtropospheric subsidence values of the order of 1 cm s⁻¹. Upward motion occurs inside 300 km. The maximum circular mean updraft, as estimated from diagnostic [Hawkins and Rubsam, 1968] and theoretical models [Rosenthal, 1970b], is of the order of 1 m s⁻¹ and occurs in the eye wall.

The horizontal winds diminish rapidly from the inner edge of the eye wall to the center of the storm and are light and variable inside the eye. The circulation from the origin to the radius of maximum wind is approximated frequently by solid rotation.

5. Moisture and Precipitation Distribution

The moisture structure of the tropical cyclone is determined primarily by the distribution of temperature and vertical motion. Because of the nearly exponential decrease of saturation vapor pressure with temperature the specific humidity is a maximum in the lowest levels and decreases rapidly with height. Figure 6 shows the mean specific humidity as a function of height observed within 222 km of the center of 92 hurricanes [Sheets, 1969]. Also shown in Figure 6 is the relative humidity profile (approximately equal to the ratio of observed to saturated specific humidity). Although the

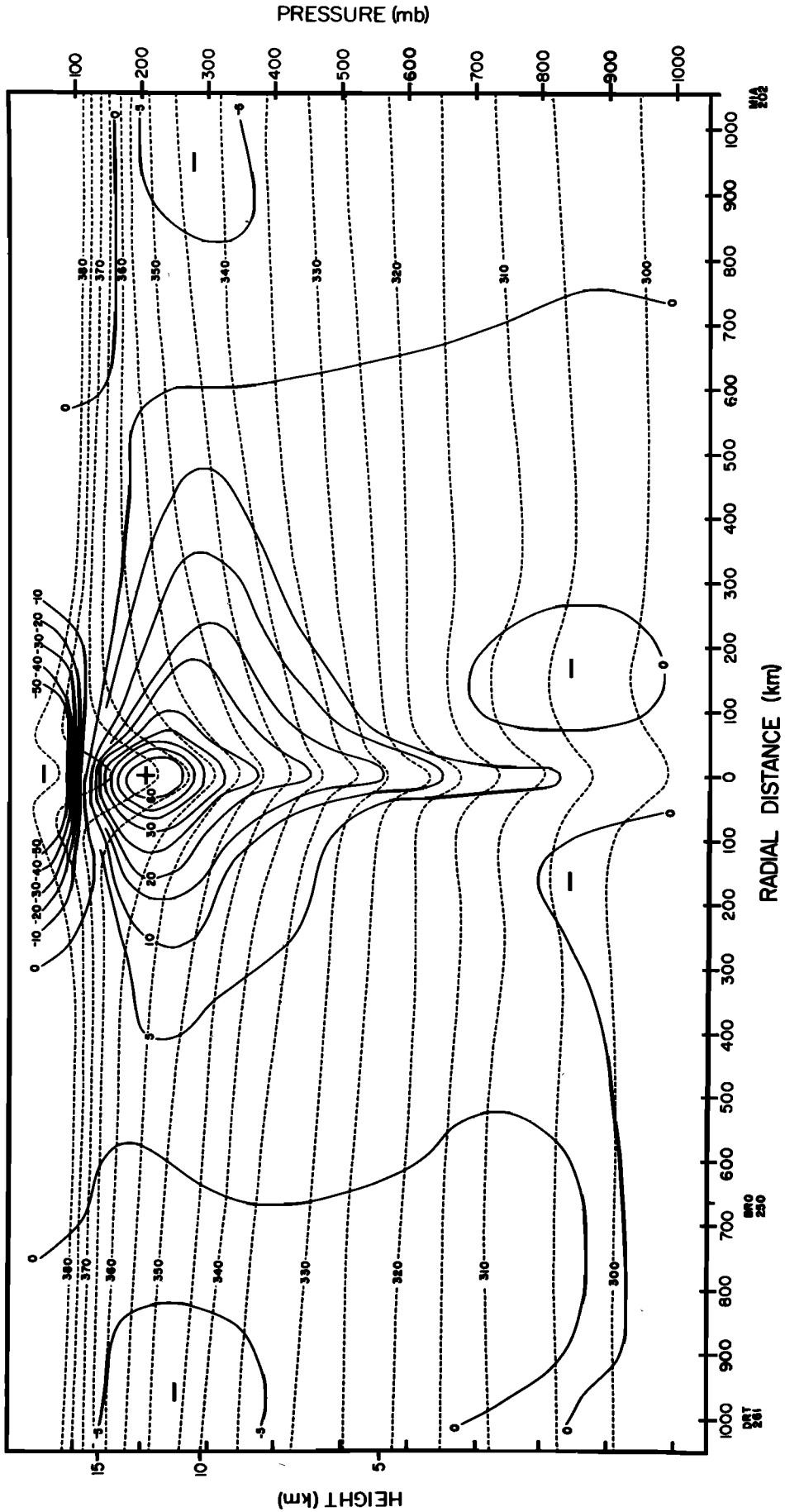


Fig. 2. Potential temperature (degrees Kelvin, dashed lines) and mass-weighted efficiency factor (solid lines) cross section through Hurricane Hilda (1964). See section D2 for definition of efficiency factor.

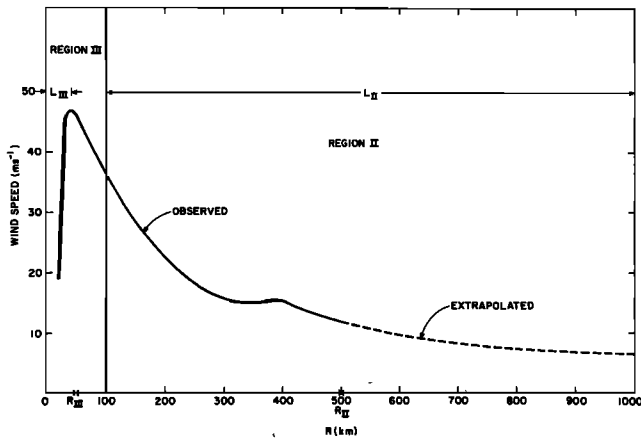


Fig. 3. Low-level wind speed profile for Hurricane Helene.

specific humidities are largely determined by the temperature structure, the relative humidities are determined mainly by the vertical motion pattern. Average values near 80% occur below 600 mbar within 222 km of the storm center, where the mean vertical velocity is upward and dense clouds are present. Beyond 300 km the subsiding air is considerably drier. The eye itself is also quite dry, middle tropospheric relative humidities sometimes being as low as 50% [Jordan, 1958]. The dry warm eye results from subsidence that produces the relatively cloud-free area in the center of the storm.

The clouds in the hurricane occur mainly in the region of mean upward motion. The dominant cloud type is convective; cumulonimbus clouds erupt in the ascending convectively unstable tropical air. The cloud bases coincide approximately with the top of the Ekman boundary layer. The many cumulonimbus clouds generate a dense cirrus canopy in the upper troposphere.

The precipitation pattern provides important clues to the relevant energetics and dynamics of tropical cyclones. Figure 7 shows a radar picture of Hurricane Cleo (1954), and Figure 5 shows a Nimbus 3 satellite photograph of Hurricane Camille (1969). Several features of the precipitation pattern are notable. The most striking is the bands that spiral anticyclonically outward from the eye wall region. These bands propagate (relative to the storm center) in a direction normal to their longitudinal axis at speeds ranging from 5 to 15 m s^{-1} . The importance of these asymmetric bands in the generation of kinetic energy and in the exchange of moisture, momentum, and heat with the larger-scale hurricane flow is not well understood, although a significant percentage of the total latent energy release occurs within the bands [Gentry, 1964].

Two other characteristics of the precipitation pattern are notable. The first important characteristic is the proportionally large area covered by radar echoes near the center, where the tropospheric temperature anomalies are positive. This latent heat release in the warm core implies a generation of available potential energy by the latent heating in this region. The rising of the warm air indicates a direct thermodynamic circulation in which total potential energy is converted to kinetic energy.

The second important characteristic of the precipitation pattern is the relatively small percentage of total area covered by active echoes. Even within the inner 200-km radius the percentage is quite small (typically less than 10% [Malkus et al., 1961]). This observation leads to the important conclusion that precipitation does not occur uniformly over the area of

mean upward motion. The occurrence of the precipitation, and the associated latent heat release in small-scale cumulonimbus convective cells rather than in a large-scale uniform pattern, is one of the most difficult aspects to treat in any hurricane model. It is impossible to resolve individual convective elements simultaneously and to determine their relation to the whole circulation. Instead hurricane modelers attempt to relate the combined effects of the many clouds to larger-scale features of the circulation. This parameterization is discussed more completely in section G2.

C. DYNAMICS OF THE TROPICAL CYCLONE

The dynamics and energetics of the hurricane are quite different from the dynamics and energetics of the larger middle-latitude atmospheric vortices. Whereas extratropical storms depend primarily on the release of energy in strong preexisting baroclinic zones associated with boundaries of distinct air masses, tropical cyclones originate and are maintained in a comparatively barotropic homogeneous environment. Although the condensation of water vapor and the release of latent heat in moist convection are of secondary importance in the extratropical cyclone, they are the main sources of energy for the hurricane. The role of the planetary boundary layer is also fundamentally different in the two cyclonic systems. Although the boundary layer processes modify the extratropical cyclone through frictional effects and varying amounts of heat and moisture addition, the cyclone is not dependent upon the boundary layer to the same extent as the hurricane is. In the hurricane the boundary layer processes are of primary importance.

Finally, the well-defined eye in the center of the storm is unique to hurricanes, and the vertical circulations associated with the eye are vital in producing the extremely low surface pressures.

A study of the distinctive hurricane dynamics and energetics, including the critical boundary layer processes of friction, evaporation, and sensible heating and the special role of the hurricane eye, may begin by a scale analysis of the dynamic and thermodynamic equations.

The equations of motion relevant to hurricane scale circulations are written in cylindrical coordinates (r, λ, z) with origin at the center of the storm. The tangential and radial equations of motion are

$$\begin{aligned} \frac{\partial v}{\partial t} + u \frac{\partial v}{\partial r} + \frac{v}{r} \frac{\partial v}{\partial \lambda} + w \frac{\partial v}{\partial z} + fu + \frac{uv}{r} \\ = -\frac{1}{\rho r} \frac{\partial p}{\partial \lambda} + \frac{1}{\rho} \frac{\partial \tau_{z\lambda}}{\partial z} + \frac{1}{\rho} \left(\frac{\partial \tau_{r\lambda}}{\partial r} + \frac{\partial \tau_{\lambda\lambda}}{r \partial \lambda} + \frac{2\tau_{r\lambda}}{r} \right) \end{aligned} \quad (3)$$

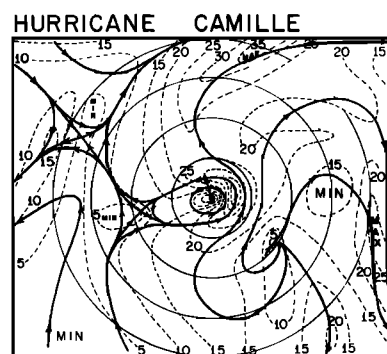


Fig. 4. Upper-level (approximately 200 mbar) streamlines (solid lines) and isotachs (knots) for Hurricane Camille (1969) showing asymmetric outflow pattern.

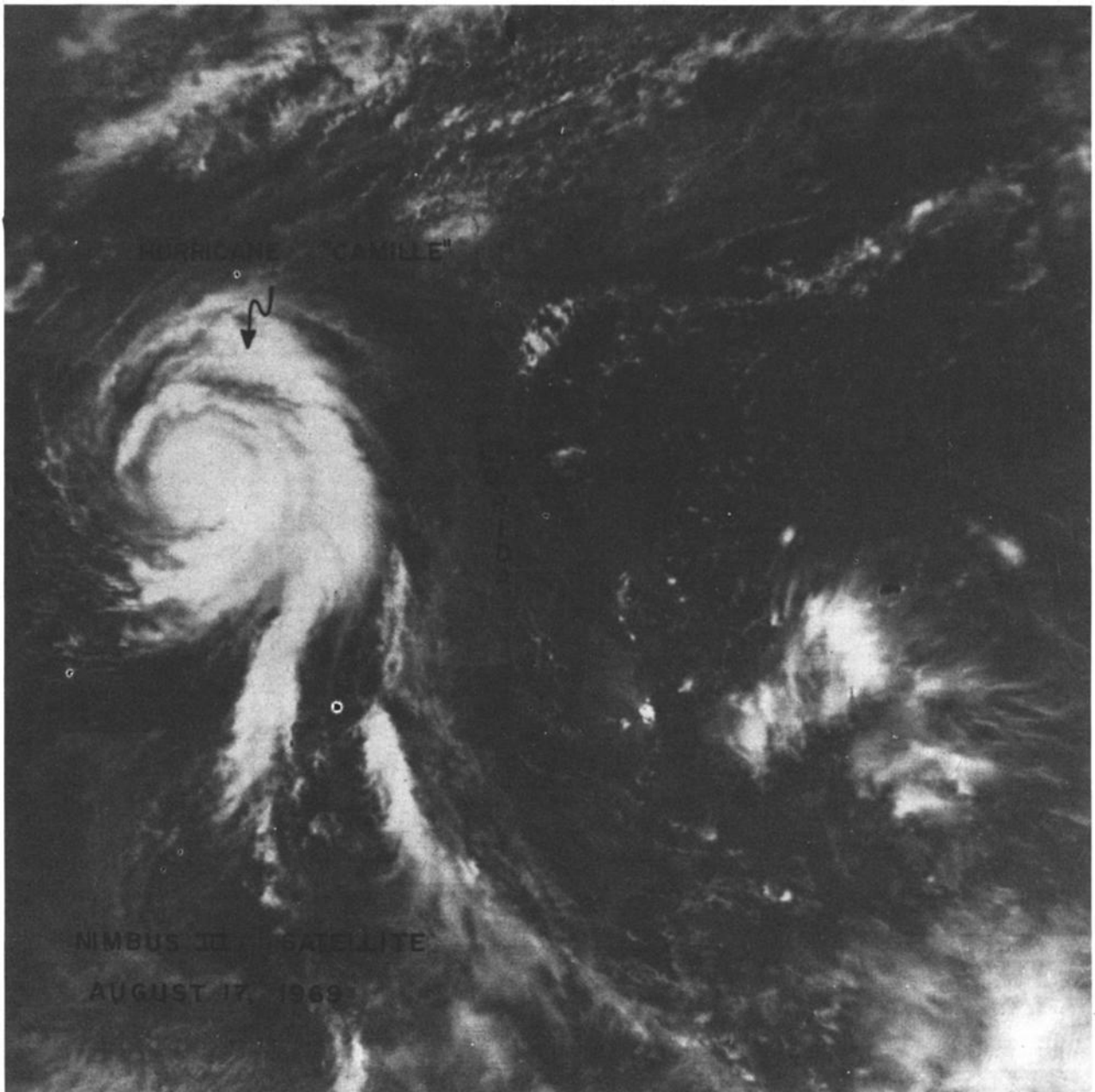


Fig. 5. Nimbus 3 satellite photograph of Hurricane Camille (1969). Note spiral band structure and relatively cloud-free environment surrounding storm. (Courtesy Peter Black, National Hurricane Research Laboratory, Miami, Florida.)

and

$$\frac{\partial u}{\partial t} + u \frac{\partial u}{\partial r} + \frac{v}{r} \frac{\partial u}{\partial \lambda} + w \frac{\partial u}{\partial z} - fv - \frac{v^2}{r} = -\frac{1}{\rho} \frac{\partial p}{\partial r} + \frac{1}{\rho} \frac{\partial \tau_{rr}}{\partial z} + \frac{1}{\rho} \left(\frac{\partial \tau_{rr}}{\partial r} + \frac{1}{r} \frac{\partial \tau_{\lambda r}}{\partial \lambda} + \frac{\tau_{rr} - \tau_{r\lambda}}{r} \right) \quad (4)$$

where the τ are the radial, tangential, and vertical eddy stresses of the v and u velocity components.

Because the vertical scale (10 km) is much less than the horizontal scale (1000 km), the hydrostatic approximation

$$\frac{\partial p}{\partial z} = -\rho g \quad (5)$$

is valid. Use of the hydrostatic relation eliminates acoustic waves, which are considered unimportant in hurricane dynamics, from the solutions in numerical models.

The continuity equation

$$\frac{\partial \rho}{\partial t} + \frac{\partial \rho u}{r \partial r} + \frac{\partial \rho v}{r \partial \lambda} + \frac{\partial \rho w}{\partial z} = 0 \quad (6)$$

may be combined with the thermodynamic equation and the hydrostatic equation to obtain a diagnostic Richardson equation for vertical velocity w . However, a simpler approach, which is followed frequently, is to neglect the local change of density $\partial \rho / \partial t$ in comparison to the divergence terms so that w may be diagnosed directly from the horizontal divergence.

The remaining equations that make up the complete set are the equation of state

$$p = \rho RT \quad (7)$$

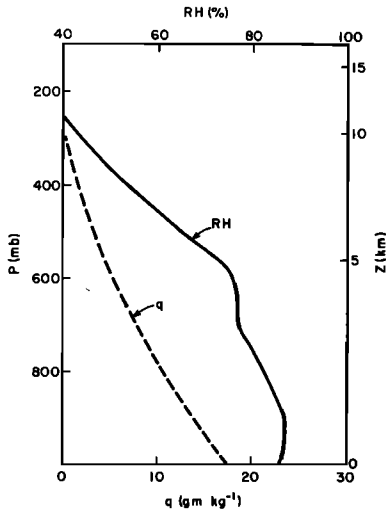


Fig. 6. Mean vertical profiles of specific humidity (q) and relative humidity (RH) from 92 hurricanes [Sheets, 1969].

the first law of thermodynamics

$$\frac{d\theta}{dt} = \frac{\theta}{C_p T} \dot{Q} + \frac{1}{r} \frac{\partial}{\partial r} \left(r K_H \frac{\partial \theta}{\partial r} \right) + \frac{\partial}{\partial z} \left(K_z \frac{\partial \theta}{\partial z} \right) + \frac{1}{r^2} \frac{\partial}{\partial \lambda} \left(K_H \frac{\partial \theta}{\partial \lambda} \right) \quad (8)$$

and a continuity equation for water

$$\frac{dq}{dt} + P - E + S = \frac{1}{r} \frac{\partial}{\partial r} \left(r K_H \frac{\partial q}{\partial r} \right) + \frac{\partial}{\partial z} \left(K_z \frac{\partial q}{\partial z} \right) + \frac{1}{r^2} \frac{\partial}{\partial \lambda} \left(K_H \frac{\partial q}{\partial \lambda} \right) \quad (9)$$

where P is precipitation (liquid water fallout), E is evaporation, and S is the storage of liquid water in the form of cloud or raindrops. The total water budget in the hurricane is extremely important and is discussed in detail in section F. In the equations (8) and (9) we have assumed that the eddy diffusivities for heat, water vapor, and momentum are equal. Equations (3)–(9) and the definition of potential temperature comprise eight equations in eight unknowns (u , v , w , p , ρ , T , θ , and q). If the diabatic heating rate \dot{Q} is related to the other variables, the system of equations is complete and can, in principle, be integrated forward in time from an initial state of the variables. However, the nonlinearity of the equations makes analytic solutions to the complete time-dependent set impossible. Attempts to obtain realistic approximate solutions are the basis for hurricane modeling, discussed in section G. In this section we present a scale analysis of the dynamics and thermodynamics in various regions of the hurricane domain to indicate the most important physical processes in each region. Before we proceed with the scale analysis, it is necessary to discuss the vertical and horizontal diffusion processes in the hurricane and to estimate the magnitude of the eddy viscosity coefficients that appear in equations (3) and (4).

1. Horizontal and Vertical Diffusion of Momentum

The vertical and horizontal eddy transport of momentum by small-scale eddies is one of the more difficult problems in understanding the dynamics of the hurricane. Both horizontal

and vertical eddy stresses are usually related to the mean horizontal and vertical shears according to the relations

$$\begin{aligned} \tau_{rr} &\approx \rho K_H \frac{\partial u}{\partial r} & \tau_{r\lambda} &\approx \rho K_H \left(\frac{\partial v}{\partial r} + \frac{\partial u}{r \partial \lambda} - \frac{v}{r} \right) \\ \tau_{\lambda\lambda} &\approx \rho K_H \left(\frac{\partial v}{r \partial \lambda} + \frac{u}{r} \right) & & \\ \tau_{zr} &\approx \rho K_z \frac{\partial u}{\partial z} & \tau_{z\lambda} &\approx \rho K_z \frac{\partial v}{\partial z} \end{aligned} \quad (10)$$

where K_z and K_H are vertical and horizontal eddy viscosity coefficients. The difficulty with this representation is that the appropriate value for K_z is known to within an order of magnitude only within the neutral boundary layer. Values for K_z in unstable boundary layers and values for K_H everywhere in the free atmosphere are speculative but are undoubtedly functions of static stability and wind shear. Above the boundary layer the ordinary vertical eddy viscosity is less important, but cumulus convection represents an important special case of vertical mixing. To estimate the order of the horizontal eddy viscosity coefficient, we must resort to simple mixing length concepts. The estimates of K_z and K_H that follow in the next section are not intended to establish numerical values for these coefficients but rather to estimate a reasonable order of magnitude so that the eddy stresses may be included in the subsequent scale analysis.

a. Vertical diffusion by small-scale turbulence. For steady unaccelerated flow in a neutral boundary layer a value for K_z appropriate to small-scale vertical eddies may be estimated from the Ekman depth $h = (2K_z/f)^{1/2}$. For an inflow layer of 1-km depth at 20°N, K_z equals 25 m² s⁻¹. However, the hurricane boundary layer is at least weakly unstable with an upward heat flux from the warm sea surface. Therefore the depth of the boundary layer is determined not only by mechanically produced turbulence but more importantly by buoyant eddies [Deardorff, 1972]. Furthermore, the flow is curved so that centrifugal effects are not negligible, at least over the inner portion of the hurricane. For example, if the mean centrifugal term v/r is included in the boundary layer equations, the modified Ekman depth is $[2K_z/(f + v/r)]^{1/2}$, and the value of K_z required to maintain an inflow layer depth of 1 km becomes considerably larger.

Because of the above difficulties in estimating K_z we include the effects of surface friction by utilizing empirical evaluations of the surface stress in hurricanes. In this technique, used by Miller [1964] and Hawkins and Rubsam [1968], the surface stress is evaluated from the observed loss of angular momentum of the inflowing air. The empirical quadratic stress law [Deacon and Webb, 1962]

$$\tau_s = \rho C_D V^2 \quad (11)$$

may then be used to evaluate the drag coefficient C_D . The assumption that the stress at the top of the boundary layer is negligibly small in comparison to the surface stress yields the estimate

$$\frac{1}{\rho} \frac{\partial \tau}{\partial z} \approx \frac{\tau_s}{h} \approx \frac{C_D V^2}{h} \quad (12)$$

Expression (12) is utilized in the scale analysis for estimating the effect of vertical diffusion in the boundary layer. Above the boundary layer the vertical diffusion of momentum by small-scale turbulence is neglected entirely.

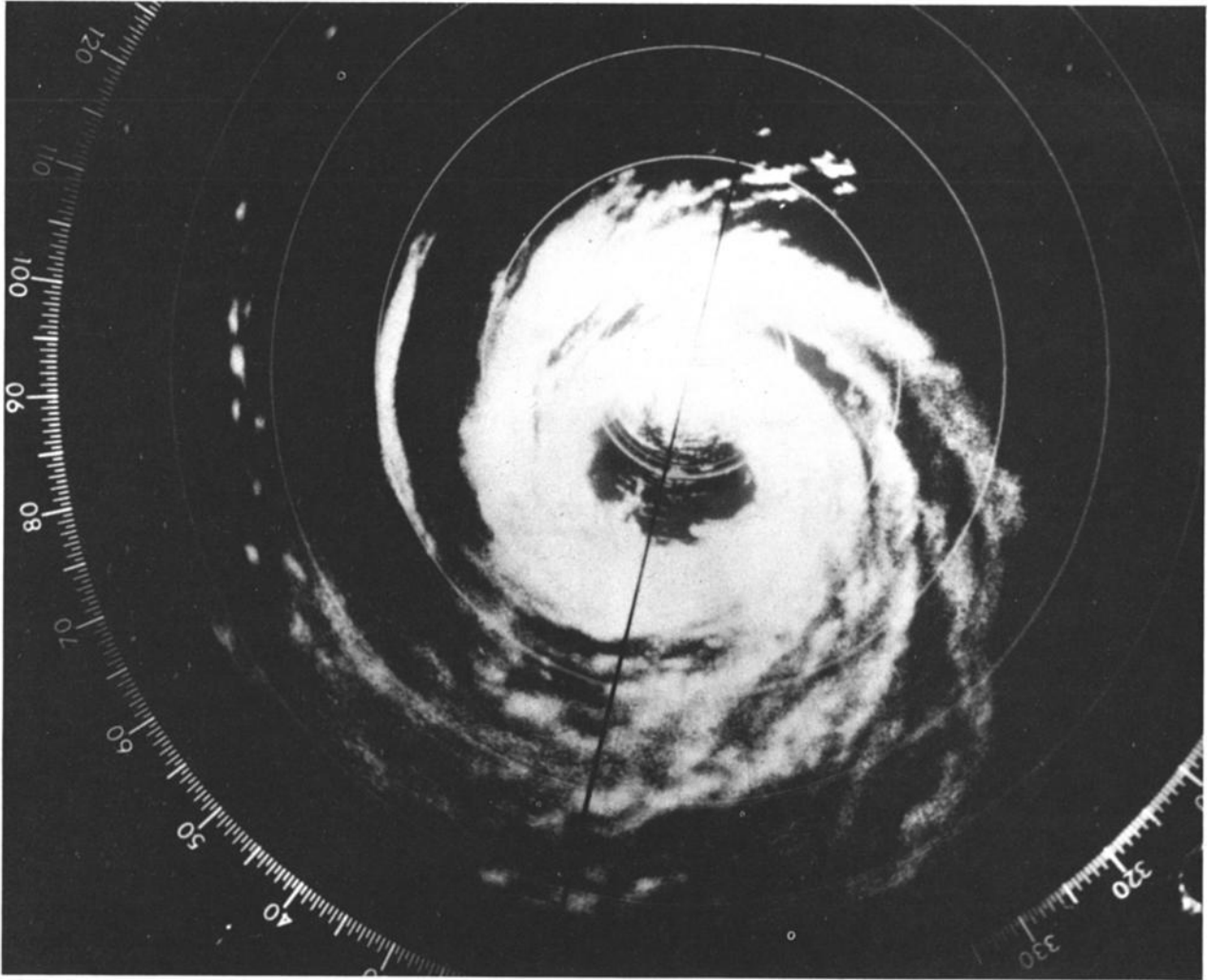


Fig. 7. Radar picture of Hurricane Cleo (1954). (Courtesy Peter Black, National Hurricane Research Laboratory, Miami, Florida.)

b. Horizontal diffusion. It is difficult to determine an appropriate value for the horizontal eddy viscosity coefficient K_H . We may estimate the order of magnitude, however, by representing K_H as the product of a typical horizontal velocity perturbation and a characteristic eddy length scale l_h corresponding to this velocity. Numerous aircraft data from hurricanes may be utilized to estimate u' and l_h . Sample radial profiles of wind speeds, derived from a sampling frequency of one observation every 2 s [Hawkins, 1962], are presented in studies by Colon *et al.* [1961], Hawkins [1962], and Sheets [1967]. In these examples, u' ranges up to 10 m s^{-1} for horizontal wavelengths of 5–40 km. If we take typical values of u' equal to 2 m s^{-1} and l_h equal to 20 km from Sheet's Hurricane Ella profiles, K_H is estimated to be of the order of $4 \times 10^4 \text{ m}^2 \text{ s}^{-1}$. Somewhat larger values may be derived from larger-scale quasi-organized eddies that are related to asymmetries in the hurricane such as a noncircular eye wall or the spiral band circulations.

c. Vertical diffusion by cumulus convection. In a warm core cyclone the thermal wind relationship implies a rapid decrease with height of the cyclonic tangential wind circulation. However, Gray [1967a] and Shea [1972] found somewhat weaker vertical shear than that expected from the thermal wind equation. They attributed the excessively strong cyclonic

winds in the upper troposphere to the upward transport of low-level cyclonic momentum by cumulus convection.

Recently, major advances in the parameterization of the vertical fluxes of heat and momentum by cumulus clouds have been made by Ooyama [1971] and Arakawa [1969]. In these studies the net vertical fluxes of heat, water vapor, and momentum are calculated as a function of statistical ensembles of cumulus elements. These recent theories promise to eliminate many of the earlier empirical and heuristic arguments regarding the effect of cumulus clouds in the larger-scale environment. However, this subject is clearly broad enough and important enough to warrant a detailed review by itself. Therefore in this paper we only estimate the order of magnitude effects of cumulus convection on the redistribution of heat, moisture, and momentum in the mature hurricane.

Representation of the vertical mixing of momentum associated with cumulus convection by an eddy viscosity coefficient is a rough approximation but yields an order of magnitude estimate of this effect [Rosenthal, 1970b]. We consider an environment occupied by a small fraction α of active cumulus convection. The stress in the x direction due to the cumulus eddy is

$$\tau_{zx} = -\rho\langle u'w' \rangle \quad (13)$$

where the average, denoted by angle brackets, is taken over an area large enough to include several clouds but small enough so that the statistical properties of the clouds and environment are constant. Horizontal momentum in the cumulus clouds is assumed to be conserved and equal to the horizontal momentum u_c at cloud base.

We wish to relate the eddy stress term to the mean vertical wind shear and an equivalent cumulus eddy viscosity K_c in the form

$$\langle u'w' \rangle = -K_c \partial(u)/\partial z \quad (14)$$

To estimate $\langle u'w' \rangle$, we note that by definition

$$\langle w \rangle = \alpha w_c + (1 - \alpha)w_e \quad (15)$$

where the subscripts c and e refer to cloud and environment, respectively. The expressions for w' inside and outside the cumulus are

$$w' = w_c - \langle w \rangle = (1 - \alpha)w_c - (1 - \alpha)w_e \quad (16)$$

and

$$w' = \alpha(w_e - w_c) \quad (17)$$

respectively. Similar expressions may be written for $\langle u \rangle$ and u' . Multiplication of the expression for $w'u'$ inside the cloud by α and the expression for $w'u'$ outside the cloud by $(1 - \alpha)$ gives

$$\begin{aligned} \langle w'u' \rangle &= \alpha(1 - \alpha)(w_e - w_c)(u_e - u_c) \\ &\approx \alpha w_c(u_c - u_e) \end{aligned} \quad (18)$$

because $\alpha \ll 1$ and $w_c \gg w_e$. Expansion of u_e in a Taylor's series produces

$$u_e \approx u_c + \partial(u)/\partial z h_c$$

where h_c is the height above cloud base. Noting that $\alpha w_c \sim \langle w \rangle$ for $w_e \sim 0$ yields an approximate expression for the eddy stress:

$$\langle w'u' \rangle \approx -\langle w \rangle h_c \partial(u)/\partial z \quad (19)$$

A comparison of (14) and (19) shows that K_c is approximately

$$K_c \sim \langle w \rangle h_c \quad (20)$$

This expression states that an equivalent vertical eddy viscosity coefficient representing cumulus momentum transport is proportional to the large-scale vertical velocity and the height above cloud base. For a value of $\langle w \rangle$ equal to 1 m s^{-1} (appropriate to the inner region of the storm's domain) and h_c equal to 5 km, K_c equals $5 \times 10^3 \text{ m}^2 \text{ s}^{-1}$, which is about 2 orders of magnitude greater than K_z .

2. Scale Analysis of Horizontal Equations of Motion

A simple scale analysis valid over the entire hurricane domain is not possible because the magnitude and shears (horizontal and vertical) of the radial and tangential components vary by more than an order of magnitude in different regions of the storm. Any subdivision of the total hurricane domain will be somewhat arbitrary. For example, a case could be made to consider the boundary layer at large and small radii, the inner eye, the eye wall region, the outflow layer at large and small radii, and the middle tropospheric layer. The dynamics in each of these regions are somewhat different. However, for simplicity, we consider only four subdivisions of the hurricane domain (Figure 8), the minimum number required to delineate the important physical processes. *Carrier et al.* [1971] utilized a similar division in a hurricane model to be described in section G. Region I is a

relatively inactive region separating the inflow (II) and outflow (IV) layers. Radial and vertical velocities are weak in region I, and the flow is expected to be in gradient balance. Region III consists of the eye and eye wall region, in which horizontal gradients are extreme and vertical motions are large. Because of the differences in the structure of these four domains each region is analyzed separately. For simplicity, axisymmetry is assumed in all four regions. For the scale analysis this assumption is equivalent to a relatively weak requirement that tangential advection, pressure, and frictional forces not exceed the corresponding radial forces in magnitude. This assumption is applicable in all regions, even though asymmetries may be present.

We let V , U , W , ΔP , ρ , L , R , H , and T be scaling parameters for tangential, radial, and vertical wind components; horizontal pressure difference; density; length scale; characteristic radial distance; depth of the region; and time scale, respectively. (Some of the notation used in the scale analysis overlaps the notation of other sections. The particular meaning of different variables will be clear from the context.)

The horizontal scale L is normally the quarter wavelength of the wave disturbance, so that a horizontal gradient such as $\partial v/\partial x$ is of the order of V/L . Because the mature hurricane does not consist of a simple wave structure, L is defined here as the minimum length over which any variable achieves its maximum and minimum values within each region of the storm. The parameter R is the mean radial distance of each domain. The definitions of L and R are illustrated in Figure 3, which shows the radial profiles of low-level wind speed in Hurricane Helene.

The tangential and radial equations of motion may be written for scaling purposes as

$$\begin{aligned} \frac{1}{fT} \left(\frac{\partial v}{\partial t} \right) + R_0 \left(u \frac{\partial v}{\partial r} \right) + R_0 \left(w \frac{\partial v}{\partial z} \right) + \frac{U}{V} \left(u \right) + \frac{U}{fR} \left(\frac{uv}{r} \right) \\ = \frac{K^*}{fH^2} \left(\frac{\partial^2 v}{\partial z^2} \right) + \frac{K_H}{fL^2} \left(\frac{\partial^2 v}{\partial r^2} \right) \end{aligned} \quad (21)$$

and

$$\begin{aligned} \frac{1}{fT} \frac{\partial u}{\partial t} + R_0 \left(u \frac{\partial u}{\partial r} \right) + R_0 \left(w \frac{\partial u}{\partial z} \right) - \frac{V}{U} (v) - \frac{V^2}{UfR} \left(\frac{v^2}{r} \right) \\ = - \frac{\Delta P}{Uf\rho L} \left(\frac{1}{\rho} \frac{\partial p}{\partial r} \right) + \frac{K^*}{fH^2} \left(\frac{\partial^2 u}{\partial z^2} \right) + \frac{K_H}{fL^2} \left(\frac{\partial^2 u}{\partial r^2} \right) \end{aligned} \quad (22)$$

where R_0 is the Rossby number U/fL and K^* is either K_z or K_c . The scaled continuity equation implies $W/H = U/L$. All quantities of equations (21) and (22) in parentheses are non-dimensional and of the order of unity.

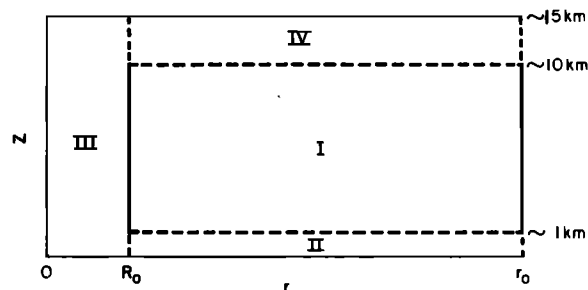


Fig. 8. Partition of hurricane into four regions. Mass inflow is significant across dashed boundaries and negligible across solid boundaries.

TABLE 1. Characteristic Values of Scaling Parameters in a Mature Tropical Cyclone

Scaling Parameters	Region I	Region II	Region III	Region IV
V , $m\ s^{-1}$	40.00	40.00	40.00	10.00
U , $m\ s^{-1}$	1.00	20.00	1.00	10.00
L , km	900.00	900.00	50.00	900.00
R , km	500.00	500.00	50.00	500.00
$W = HU/L$, $m\ s^{-1}$	0.01	0.02	0.20	0.05
H , km	10.00	1.00	10.00	5.00
$\Delta P/L$, mbar $(100\ km)^{-1}$	5.00	5.00	40.00	0.50
$K_c \sim WH$, $m^2\ s^{-1}$	100.00	...	2000.00	...
ρ , metric tons m^{-3}	1×10^{-3}	1×10^{-3}	1×10^{-3}	0.4×10^{-3}

$f \approx 5 \times 10^{-5}\ s^{-1}$, $K_H \approx 4 \times 10^4\ m^2\ s^{-1}$, and $C_D \approx 0.002$ in all four regions.

Characteristic values of the scaling parameters, based upon observations, are listed by region in Table 1. Table 2 lists the magnitudes of the nondimensional coefficients for each term in the radial and tangential equations of motion. The time scale T for each variable in each region may be estimated by assuming that $(fT)^{-1}$ is of the same order as the maximum nondimensional coefficient in the equation. This estimate will be too small if there is a balance of the large terms in the equation. For example, such a balance exists between the centripetal, the pressure gradient, and the Coriolis forces in the

radial wind equation, and therefore a time scale estimate is not made for the radial wind component.

Disregarding all terms at least an order of magnitude smaller than the largest term in each equation, we arrive at the lowest-order approximation to the equations of motion in each region. In the inactive region I, the only terms that may be neglected in the tangential wind equation are the vertical and horizontal eddy viscosity terms. Furthermore, all coefficients are small, so that v is slowly varying in this region with a time scale of several days. Thus in the absence of large-

TABLE 2. Magnitude of Nondimensional Coefficients of the Terms in the Tangential and Radial Equations of Motion and in the Thermodynamic Equation for Various Regions in a Mature Tropical Cyclone

Tangential Equation of Motion*								
Region	T	$\frac{1}{fT}$	R_0	$\frac{U}{V}$	$\frac{U}{fR}$	$\frac{K_c}{fH^2}$	$\frac{K_H}{fL^2}$	$\frac{C_D V}{fH}$
I	6 days	0.02	0.02	0.025	0.04	0.02	10^{-3}	...
II	6 hours	0.80	0.40	0.500	0.80	...	10^{-3}	1.6
III	12 hours	0.40	0.40	0.025	0.40	0.40	0.32	...
IV	6 hours	0.80	0.20	1.000	0.40	...	10^{-3}	...
Radial Equation of Motion†								
Region	R_0	$\frac{V}{U}$	$\frac{V^2}{Ufr}$	$\frac{-\Delta P}{Uf\rho L}$	$\frac{K_c}{fH^2}$	$\frac{K_H}{fL^2}$	$\frac{C_D V}{fH}$	
I	0.02	40.0	64.0	100.0	0.02	10^{-3}	...	
II	0.40	2.0	3.2	5.0	...	10^{-3}	1.6	
III	0.40	40.0	640.0	800.0	0.40	0.32	...	
IV	0.20	1.0	0.4	2.5	...	10^{-3}	...	
Thermodynamic Equation‡								
Region	T	$\frac{1}{fT}$	R_0	$R_0 \left(1 + \frac{\partial}{\partial \theta}\right)$	$-\frac{1}{f\theta} \frac{d\theta}{dt}$	$\frac{K_z}{fH^2} \left(1 + \frac{\partial}{\partial \theta}\right)$	$\frac{K_H}{fL^2}$	
I	1 day	0.20	0.02	0.10	0.20	0.025	10^{-3}	
II	8 hours	0.60	0.40	0.60	0.20	0.200	10^{-3}	
III	2 hours	2.00	0.40	2.00	2.00	0.020	0.32	
IV	1 day	0.20	0.20	0.40	0.04	0.020	10^{-3}	

Region I is the middle troposphere, II the boundary layer, III the eye wall, and IV the outflow.

* The tangential equation of motion is

$$\frac{1}{fT} \left(\frac{\partial v}{\partial t} \right) + R_0 \left(u \frac{\partial v}{\partial r} \right) + R_0 \left(w \frac{\partial v}{\partial z} \right) + \frac{U}{V} (u) + \frac{U}{fR} \left(\frac{uv}{r} \right) = \frac{K_c}{fH^2} \left(\frac{\partial^2 v}{\partial z^2} \right) + \frac{K_H}{fL^2} \left(\frac{\partial^2 v}{\partial r^2} \right) + \frac{C_D V}{fH} (v)$$

† The radial equation of motion is

$$\frac{1}{fT} \left(\frac{\partial u}{\partial t} \right) + R_0 \left(u \frac{\partial u}{\partial r} \right) + R_0 \left(w \frac{\partial u}{\partial z} \right) - \frac{V}{U} (v) - \frac{V^2}{UfR} \left(\frac{v^2}{r} \right) = \frac{-\Delta P}{Uf\rho L} \left(\frac{1}{\rho} \frac{\partial p}{\partial r} \right) + \frac{K_c}{fH^2} \left(\frac{\partial^2 u}{\partial z^2} \right) + \frac{K_H}{fL^2} \left(\frac{\partial^2 u}{\partial r^2} \right) + \frac{C_D V}{fH} (u)$$

‡ The thermodynamic equation is

$$\frac{1}{fT} \left(\frac{\partial \theta}{\partial t} \right) + R_0 \left(u \frac{\partial \theta}{\partial r} \right) + R_0 \left(w \frac{\partial \theta}{\partial z} \right) = -\frac{1}{f\theta} \frac{d\theta}{dt} + \frac{K_z}{fH^2} \left(1 + \frac{\partial}{\partial \theta} \right) \left(\frac{\partial^2 \theta}{\partial z^2} \right) + \frac{K_H}{fL^2} \frac{\partial^2 \theta}{\partial r^2}$$

scale interactions with extratropical systems that would invalidate the scale analysis the middle-tropospheric tangential circulation will be very slow to decay when tropical storms move over land. The radial equation of motion in region I reduces to the gradient wind equation

$$\frac{V}{U}(v) + \frac{v^2}{UfR} \left(\frac{v^2}{r} \right) = \frac{\Delta P}{Uf\bar{\rho}L} \left(\frac{1}{\rho} \frac{\partial p}{\partial r} \right) \quad (23)$$

which indicates the balanced nature of the flow in this region.

In the boundary layer (region II), only horizontal diffusion and the effects of cumulus convection are negligible in both equations. The vertical diffusion of momentum, represented by the stress at the ocean-air interface, is balanced by the centrifugal, Coriolis, and pressure gradient terms. The winds therefore are subgradient, and the air is accelerated inward toward lower pressure. As is discussed more completely in section D1, this acceleration represents the primary generation of kinetic energy in the hurricane. The time scale for the tangential wind in the boundary layer is of the order of only a few hours, in marked contrast to the much longer time scale of the slowly varying middle-tropospheric region. Thus the adjustment of the wind field in the lowest kilometer of the hurricane circulation will be quite rapid when the hurricane moves from water to land or vice versa.

The scale analysis of the radial wind equation in the outflow layer (region IV) suggests that the gradient wind equation holds within 10%. Because of the significant outward radial flow in this region the time scale of the tangential wind variation is about 6 hours, which is much shorter than the time scale in the middle troposphere, where radial motions are weak.

An interesting balance of forces that is not present in extratropical cyclones exists in the vicinity of the eye and eye wall (region III). Whereas advection and diffusion may be neglected in the radial equation of motion, so that only the gradient wind equation is left, the horizontal and cumulus diffusion terms and the inertial terms contribute substantially in the tangential wind equation. The importance of horizontal eddy diffusion is especially notable, since horizontal turbulence is usually negligible in comparison to vertical turbulence. In the time-dependent problem the tangential wind v is sensitive to K_H , and so we also expect the radial flow u to be strongly affected through the v^2/r term. Because small variations in u may greatly affect the low-level moisture convergence and the condensational heating rate, it is clear that horizontal diffusion is important, even though the gradient wind balance is valid to within an order of magnitude.

3. Dynamics of the Hurricane Eye

The dynamics of the hurricane eye and eye wall region (III) are less well understood than the dynamics of the other regions of the hurricane. Considerably more effort should be devoted toward understanding the processes that generate and maintain the eye because the eye is more than just a curiosity associated with the hurricane. The subsidence and associated dry adiabatic warming inside the eye allow much lower central pressures, and therefore stronger maximum winds, than would be possible with simply moist adiabatic ascent of low-level air. The importance of the eye may be seen in the strong coincidence between the stage of tropical storm development and the structure of the eye [Jordan, 1961]. Extremely warm dry eyes are almost exclusively associated with intensifying storms. During the weakening stage the eye soundings are much closer to the moist adiabatic lapse rate.

The dynamics of the eye and eye wall can be investigated by considering the angular momentum and energy budgets of air flowing toward the center of the storm [Kuo, 1958]. The essential physics is summarized by considering an adiabatic and frictionless vortex and then modified for a more realistic applicability to the hurricane.

For steady, adiabatic, and inviscid flow the total energy H is conserved according to the Bernoulli equation

$$H = c_p T + gz + k = \text{const} \quad (24)$$

where $c_p T$ is the enthalpy, gz is the potential energy, and k is the kinetic energy. The absolute angular momentum ($rv + fr^2/2$) and potential temperature θ are also conserved along any streamline. The conservation of angular momentum of the inflowing air requires that the tangential wind speed increase as the inverse of radial distance from the storm center. However, the finite amount of total energy limits the maximum achievable wind speed. Therefore the inflowing current may not penetrate beyond some small radius but must turn upward and outward. Calculation by (24) and the conservation of angular momentum of this innermost radius, which may be identified as the radius of the eye wall, yields values larger than observed eye radii. The discrepancy is primarily a result of the neglect of angular momentum loss to the sea. In the more realistic case in which surface frictional effects are considered, the loss of angular momentum allows inflowing air to reach smaller radii and still satisfy the energy constraint. Thus the radius of the eye wall is determined by the original values of the air's total energy and absolute angular momentum and by subsequent changes in these quantities along the trajectory.

The production of subsidence inside the eye may be explained as a consequence of the presence of supergradient winds in the vicinity of the eye wall at radii less than the radius of maximum wind, as was proposed by Malkus [1958] and Kuo [1958]. The outward acceleration that results from the supergradient winds in the eye produces a mean outward radial acceleration and a compensating sinking of air in the eye.

Adiabatic subsidence of air without mixing from the upper troposphere to levels near the surface would produce excessively warm and dry soundings in the eye. For example, undiluted descent from 200 mbar to 800 mbar of a parcel with initial temperature and humidity equal to those of the mean hurricane sounding [Sheets, 1969] would produce an 800 mbar temperature and humidity of 57°C and near 0%, respectively. However, observed values [Jordan, 1958] of temperature and humidity are about 19.0°C and 89%, respectively. Malkus [1958] showed that a realistic temperature and humidity structure in the eye could be produced by lateral mixing of the descending air with cooler moist air originating in the convective eye wall. The evaporation of liquid water reduces the compressional warming and increases the humidity of the subsiding air.

At least two, not necessarily contradictory, explanations exist for the supergradient winds that are responsible for the eye subsidence. According to the first hypothesis, proposed by Malkus [1958] and Kuo [1958], the supergradient winds are generated by the horizontal diffusion of excessive tangential momentum inward from the radius of maximum wind. The large horizontal shear in the vicinity of the eye wall favors the development of eddies and strong lateral mixing. Proof that mixing does occur is shown by the observed temperature and humidity in typical eye soundings as discussed above. To

determine the sign of the transport of angular momentum by these eddies, we consider the mean tangential wind structure of the hurricane eye.

The horizontal diffusion F_λ of tangential momentum may be written

$$F_\lambda = K_H \left(\frac{\partial^2 v}{\partial r^2} + \frac{1}{r} \frac{\partial v}{\partial r} - \frac{v}{r^2} \right) \quad (25)$$

The sign of the eddy transport depends on the radial profile of the mean tangential wind. Examination of composite radial profiles of v inside the radius of maximum wind [Shea, 1972, pp. 25–26] shows that the curvature of the tangential wind profile yields a positive value for F_λ at all levels (900, 750, 650, 525, and 240 mbar). Thus horizontal diffusion of tangential momentum is the correct sign to account for the supergradient winds.

An alternative explanation of the supergradient winds involves the overshooting of inflowing air parcels beyond the point of zero acceleration and the sudden deceleration that occurs as r becomes small. To show how steady state supergradient winds may exist in the boundary layer, where surface friction is important, we consider the radial equation of motion in the form

$$\frac{du}{dt} + \frac{C_D |V|}{h} u = f(v - v_{gr}) + \frac{1}{r}(v^2 - v_{gr}^2) \quad (26)$$

where v_{gr} is the gradient wind and h is the depth of the boundary layer. For inflow ($u < 0$) the air must be decelerating ($du/dt > 0$) for v to be supergradient. For axisymmetric steady flow the deceleration is

$$du/dt = u \partial u / \partial r = (\partial u^2 / 2) / \partial r \quad (27)$$

Thus steady state supergradient flow in the inflow layer may exist only if u^2 decreases toward the center, i.e., inside the radius of zero inward acceleration. Observations [Shea, 1972] confirm the close correspondence between decreasing inward radial flow and supergradient winds.

The supergradient winds above the boundary layer in the vicinity of the eye wall may be explained by the vertical transport of tangential momentum by cumulus clouds. Because of the storm's warm core the pressure gradient decreases upward. However, the air in the eye wall rises sufficiently rapidly that in spite of frictional effects, enough tangential momentum is conserved so that the air remains supergradient at higher levels.

Of course, both of the above processes may contribute to the production of the supergradient winds. Further observational and modeling studies are needed to ascertain the relative importance of each process.

4. Scale Analysis of Thermodynamic Equation

The thermodynamic equation (8) for an axisymmetric hurricane is

$$\begin{aligned} \frac{\partial \theta}{\partial t} + u \frac{\partial \theta}{\partial r} + w \frac{\partial \theta}{\partial z} \\ = \frac{\theta}{C_p T} \dot{Q} + \frac{1}{r} \frac{\partial}{\partial r} r \left(K_H \frac{\partial \theta}{\partial r} \right) + \frac{\partial}{\partial z} \left(K_z \frac{\partial \theta}{\partial z} \right) \end{aligned} \quad (28)$$

We write θ in the form

$$\theta = \bar{\theta} \theta_1'(z) + \hat{\theta} \theta_2'(r, z, t) \quad (29)$$

where $\theta_{1,2}'$ are nondimensional and of the order of 1. The first term in (29) represents the distribution of θ with height in the mean hurricane environment, and the second term represents the potential temperature perturbation associated with the hurricane. The scaled nondimensional thermodynamic equation may then be written

$$\begin{aligned} \frac{1}{f\bar{\theta}} \left(\frac{\partial \theta}{\partial t} \right) + R_0 \left(u \frac{\partial \theta}{\partial r} \right) + R_0 \left[1 + \frac{\bar{\theta}}{\hat{\theta}} \right] \left(w \frac{\partial \theta}{\partial z} \right) \\ = \frac{1}{f\hat{\theta}} \frac{d\theta}{dt} + \frac{K_z}{fH^2} \left[1 + \frac{\bar{\theta}}{\hat{\theta}} \right] \left(\frac{\partial^2 \theta}{\partial z^2} \right) + \frac{K_H}{fL^2} \left(\frac{\partial^2 \theta}{\partial r^2} \right) \end{aligned} \quad (30)$$

where the primes have been dropped from θ and all terms in parentheses are nondimensional and of the order of unity. The departure of potential temperature $\hat{\theta}$ from the mean environmental temperature is of the order of 10°C. The mean increase in potential temperature $\bar{\theta}$ over the depth H of each region is listed in Table 3.

The material time rate of change of potential temperature that results from diabatic heating or cooling processes is represented by the term $(1/f\hat{\theta}) d\theta/dt$. The possibly important sources and sinks of heat are (1) latent heat of condensation, (2) sensible heat addition at the air-sea interface, (3) flux divergence of infrared radiation, and (4) direct absorption of solar radiation. In our estimation of the magnitude of these four diabatic processes we denote the time rates of change of θ due to the first two by $(d\theta/dt)_L$ and $(d\theta/dt)_S$, respectively, and the rate of change due to the net effect of the two radiative processes by $(d\theta/dt)_R$.

a. Condensation heating. The release of latent heat in the cumulus convection and the subsequent interactions with the environment are complex processes and are discussed in section G. In this section the order of magnitude is estimated in regions I and III from observed rainfall rates. Here diabatic heating associated with the condensation of water vapor should be carefully distinguished from any net sensible warming of the environment. As was shown by Gray [1972], the effect of cumulus convection is frequently to cool rather than warm the immediate environment of the cloud. This paradox

TABLE 3. Magnitude of the Rates of Change of Potential Temperature Due to Diabatic Heating Processes for Various Regions in a Mature Tropical Cyclone

	Region I (Middle Troposphere)	Region II (Boundary Layer)	Region III (Eye Wall)	Region IV (Outflow Layer)
$\bar{\theta}$, °C	40.0	4.0	40.0	10.0
$[1 + (\bar{\theta}/\hat{\theta})]$	5.0	1.4	5.0	2.0
$(d\theta/dt)_L$, °C d ⁻¹	9.0	...	90.0	...
$(d\theta/dt)_S$, °C d ⁻¹	...	9.0
$(d\theta/dt)_R$, °C d ⁻¹	2.0	2.0	...	2.0
$(1/f\hat{\theta})(d\theta/dt)_{\max L, S, R}$	0.20	0.20	2.00	0.04

The value of $\hat{\theta}$ is 10°C for all regions in these estimates.

results from the fact that most of the local temperature increase due to condensation is offset by the upward transport of air with much lower potential temperature. Thus the diabatic heating rate is nearly canceled by the adiabatic cooling term.

Although some of the water vapor that condenses in rising air parcels reevaporates at the cloud edges and yields no net diabatic heating within the column, we may estimate the order of magnitude of the net latent heating rate from observed rainfall rates. The mean heating rate in a layer of pressure depth ΔP is related to the rainfall rate according to

$$\dot{Q} = (gL/\Delta P)R \text{ erg s}^{-1} \text{ g}^{-1} \quad (31)$$

where g , L , and ΔP are expressed in cgs units and R is given in centimeters of rain per second. Typical areal averages of rainfall rates for the eye wall region and the region from the outer edge of the eye wall to the edge of the cloud cover are 30 and 3 cm/d, respectively. These rainfall rates yield

Region I

$$(d\theta/dt)_L \sim \dot{Q}/c_p \sim 10^{-4} \text{ }^\circ\text{C s}^{-1} \quad (32a)$$

Region III

$$(d\theta/dt)_L \sim \dot{Q}/c_p \sim 10^{-3} \text{ }^\circ\text{C s}^{-1} \quad (32b)$$

b. Sensible heating. Because of the large heat capacity of water compared to that of air the ocean acts as an effective source of heat when the air is cooler than the sea surface. The rate of sensible heating may be estimated following *Byers'* [1944] and *Riehl's* [1954] argument. The air temperature at large distances from the storm center is nearly equal to the sea temperature. As air spirals in toward lower pressure, cooling would result due to expansion if no diabatic heating were present. However, observations show only a small temperature decrease near the storm center, indicating that heat has been added to the inflowing air. The magnitude of the required sensible heating is estimated from the first law of thermodynamics for an isothermal process,

$$\left(\frac{d\theta}{dt}\right)_s \sim -\kappa \frac{\theta}{p} \frac{dp}{dt} \quad (33)$$

For an average inflow velocity of 10 m s^{-1} a parcel requires $5 \times 10^4 \text{ s}$ to reach the center of the storm from a distance of 500 km. For a typical pressure drop of 70 mbar, $(d\theta/dt)_s$ is approximately $10^{-4} \text{ }^\circ\text{C s}^{-1}$.

c. Infrared radiative cooling and absorption of solar radiation. Emission of infrared radiation by carbon dioxide and water vapor in the troposphere normally produces a flux divergence of energy and a net cooling effect. In the clear tropical environment surrounding the hurricane, infrared cooling exceeds the direct absorption of solar radiation, and both theory and observations show a rather uniform vertical distribution of cooling of about 2°C d^{-1} . Although strong infrared cooling and heating may occur in thin layers above and below layered clouds, respectively, the difference between infrared emission and absorption of shortwave solar radiation is negligible in the interior region, where thick multilevel clouds occur. Therefore the only significant radiative loss of energy occurs in the clear hurricane environment (the outer portion of region I), where $(d\theta/dt)_R$ is about $2 \times 10^{-5} \text{ }^\circ\text{C s}^{-1}$.

The magnitudes of the rates of change of potential temperature due to the diabatic heating processes are listed by

region in Table 3. The scaling coefficients in the thermodynamic equation are listed in Table 2. In the middle troposphere (region I) a balance exists between adiabatic vertical motion and diabatic heating, horizontal advection and diffusion of heat contributing only slightly. In the inner portion of region I, cooling associated with the mean upward motion is balanced by the release of latent heat, whereas in the clear outer part of the region the balance is between dry adiabatic warming associated with weak subsidence and net radiative cooling. The processes are all weak in this region, so that the time scale is no shorter than about 1 day.

In the boundary layer (region II), horizontal and vertical advection, sensible heating, and vertical diffusion of heat all contribute substantially to thermodynamic balance. Only horizontal diffusion is negligible. Because of the stronger radial motions the time scale may be shorter (on the order of 8 hours) here than in the middle troposphere.

In the eye and eye wall region the major thermodynamic balance is achieved through the compensating effect of the strong latent heating and vertical motion, as was noted earlier. However, horizontal advection and diffusion may not be entirely negligible because of the large horizontal temperature gradients. The time scale for temperature changes in this central region may be quite short, on the order of an hour, because of the large magnitudes of the vertical advection and latent heating terms.

The outflow layer (region IV) is the only region in the hurricane where the flow is approximately isentropic. Here the potential temperature is determined by horizontal and vertical advection, which dominate infrared cooling and the diffusion of heat.

D. ENERGETICS OF THE TROPICAL CYCLONE

We next consider the production of kinetic energy necessary to maintain the extreme winds against the continuous drain of kinetic energy by surface friction and internal mixing in the free atmosphere. The principal mechanism by which internal and potential energy (or available potential energy) are converted to kinetic energy is the acceleration of air toward low pressure in the inflow layer. The maintenance of the reservoir of available potential energy against this conversion must be related to the diabatic heating processes in order to complete the energy cycle.

The energetics of a self-sustained thermally driven hurricane may be summarized as follows. Differential heating maintains the baroclinity and the store of available potential energy. Available potential energy is converted to kinetic energy in the inflow layer, where friction causes the winds to accelerate toward lower pressure. In the steady state this production of kinetic energy is offset by frictional dissipation, both in the boundary layer and in the free atmosphere, leaving little kinetic energy left over for export out of the hurricane domain. On the other hand, the horizontal transport of heat away from the warm core helps maintain the baroclinic structure and appears as a positive term in the available potential energy equation. The next sections illustrate these processes quantitatively and present energy budgets from a model and several real hurricanes.

1. Kinetic Energy Budget

The kinetic energy equation for the hurricane may be obtained by multiplying equations (3) and (4) by v and u , re-

spectively, adding, and making use of the continuity equation (6):

$$\begin{aligned} \frac{\partial \rho k}{\partial t} + \frac{\partial r \rho u k}{r \partial r} + \frac{\partial \rho v k}{r \partial \lambda} + \frac{\partial w \rho k}{\partial z} \\ = -\frac{v}{r} \frac{\partial p}{\partial \lambda} - u \frac{\partial p}{\partial r} + \rho \mathbf{V} \cdot \mathbf{F} \end{aligned} \quad (34)$$

where \mathbf{F} represents the vector sum of various frictional forces. Integration of equation (34) over the volume defined by $0 \leq z \leq H$ and $0 \leq r \leq r_0$ and the condition that $w(z=0) = w(H) = 0$ yield the kinetic energy budget for the hurricane volume:

$$\begin{aligned} \frac{\partial K}{\partial t} = - \int_0^H \int_0^{r_0} r_0 (\rho u k)_{r_0} d\lambda dz \\ + \int_0^H \int_0^{r_0} \int_0^{2\pi} \left(-\frac{v}{r} \frac{\partial p}{\partial \lambda} - u \frac{\partial p}{\partial r} \right. \\ \left. + \rho \mathbf{V} \cdot \mathbf{F} \right) r d\lambda dr dz \end{aligned} \quad (35)$$

The first term on the right of (35) is the vertically integrated horizontal flux of kinetic energy across the outer radius r_0 . For large domains (radius greater than 1000 km) this term is probably negligible, since the vertical wind shear is small in the hurricane environment [Gray, 1967a]. Palmén and Jordan [1955] showed from mean data that the net inflow of k across the 666-km radius is very small. If $k(r_0)$ were identically constant, the only contribution from this term would be from the net mass divergence in the volume, a very small quantity on this scale. In any case, hurricane development is not dependent upon an outside source of kinetic energy, as is shown by numerical models [Ooyama, 1969; Rosenthal, 1970b] in which the boundary flux of kinetic energy is about 1% of the production of kinetic energy within the volume.

The terms $v/r \partial p/\partial \lambda$ and $u \partial p/\partial r$ in (35) represent the conversion of potential and internal energy to kinetic energy by cross-isobar flow. To estimate the conversion from the tangential component, we let

$$v = \langle v \rangle^\lambda + v' \quad p = \langle p \rangle^\lambda + p' \quad (36)$$

where

$$\langle \quad \rangle^\lambda = \frac{1}{2\pi} \int_0^{2\pi} (\quad) d\lambda \quad (37)$$

and the prime represents a deviation from this mean. Then the net contribution to the kinetic energy budget by the tangential wind component is

$$- \int_0^H \int_0^{r_0} \int_0^{2\pi} v' \frac{\partial p'}{\partial \lambda} d\lambda dr dz \quad (38)$$

In the lower and middle troposphere, where the isobars are nearly circular and p' is small, this contribution is probably negligible. In the outflow layer the horizontal pressure gradient is weak if not symmetric, so that this term is small in the upper troposphere as well. A region in which this eddy conversion may be large locally is in the vicinity of the eye wall, where significant variations from a circular eye structure have been observed. However, the eye represents a very small area relative to the entire domain, and the integrated effect of this term is negligible.

The important source of kinetic energy production in the hurricane is the radial flow toward lower pressure in the inflow layer, represented by $u \partial p/\partial r$. This inflow is a result of

surface friction, which reduces the tangential wind speed and thereby destroys the gradient balance, so that the inward pressure gradient force exceeds the Coriolis and centripetal forces. In the warm core low the maximum pressure gradient ($\partial p/\partial r < 0$) occurs at the lowest level, at which the inflow ($u < 0$) is maximum. In the outflow layer, where the radial flow is reversed, the pressure gradient is much weaker. The result is a net production of kinetic energy, dominated by the contribution from the inflow region.

A substantial dissipation of kinetic energy in the hurricane occurs in the boundary layer through turbulent diffusion and ultimate loss of energy to the sea surface. Empirical evidence [Hawkins and Rubsam, 1968] also indicates that dissipation of kinetic energy outside the boundary layer by vertical and horizontal eddies, including cumulus convection, is roughly equal to that inside the boundary layer. Since the kinetic energy production occurs mainly within the boundary layer whereas substantial dissipation occurs outside the boundary layer, the boundary layer must be responsible for a net gain of kinetic energy. Thus we have the paradox that surface friction is responsible for a net increase in kinetic energy and without friction the hurricane could not exist.

It also follows that a linear decrease of pressure with decreasing radius is not sufficient to allow the wind speed to increase inward in a balanced state over the effects of friction. To prove this statement, we consider a balance between the centripetal, the Coriolis, and the frictional forces and neglect variations in density:

$$\frac{v^2}{r} + fv = \frac{1}{\rho_0} \frac{\partial p}{\partial r} + K_z \frac{\partial^2 v}{\partial z^2} \quad (39)$$

Differentiation with respect to radius yields

$$\left(\frac{2v}{r} + f \right) \frac{\partial v}{\partial r} = \frac{1}{\rho_0} \frac{\partial^2 p}{\partial r^2} + \frac{v^2}{r^2} + \frac{\partial}{\partial r} \left(K_z \frac{\partial^2 v}{\partial z^2} \right) \quad (40)$$

In order that v increase inward the inequality

$$\frac{1}{\rho_0} \frac{\partial^2 p}{\partial r^2} < - \left[\frac{v^2}{r^2} + \frac{\partial}{\partial r} \left(K_z \frac{\partial^2 v}{\partial z^2} \right) \right] \quad (41)$$

must be satisfied. If v increases with decreasing radius, the radial derivative of the frictional force is positive, so that the right side of inequality (41) is negative. In other words the radial pressure gradient must increase with decreasing radius in order that the wind speed increase. As Figure 1 indicates, the radial profile of surface pressure is nearly exponential with radial distance.

2. Available Potential Energy Budget

The preceding section suggests that the conversion of total potential energy, defined as the sum of potential and internal energy, to kinetic energy in the mature hurricane approximately balances the sum of all dissipative effects and thus there is little net exchange of kinetic energy with the environment. To complete a consistent energy budget of the tropical cyclone, it is necessary to consider how diabatic processes maintain the total potential energy that is continually converted to kinetic energy.

The relation of heating and cooling to the maintenance of the total potential energy field may be examined from the available potential energy viewpoint. The available potential energy concept originates with Margules [1903], who differentiated between the vast quantity of potential and internal

energy that exists in the atmosphere and the relatively small percentage that may be converted to kinetic energy. For example, a hydrostatic barotropic fluid with no horizontal pressure gradients possesses considerable potential and internal energy, but no conversion to kinetic energy is possible.

The minimum total potential energy of a particular state of the atmosphere is obtained by an isentropic redistribution of mass to a hydrostatic barotropic atmosphere in which the pressure of each isentropic surface equals the mean pressure of that surface. Departures from this state represent energy that is available for conversion to kinetic energy, i.e., available potential energy. Thus baroclinity is closely associated with available potential energy, and diabatic processes that tend to create or maintain baroclinic fields generate available potential energy.

The available potential energy concept has most often been applied in the study of global atmospheric energetics [Lorenz, 1955; Dutton and Johnson, 1967]. Recently, Johnson [1970] extended the theory to limited regions of the earth. The hurricane is perhaps the best example of an isolated thermally driven circulation, and the concept of available potential energy on this limited scale has proved useful. The hurricane may be considered analogous to a heat engine driven by differential heating and cooling. The theory of available potential energy demonstrates the links between heating, maintenance of the baroclinity, and conversion of available potential to kinetic energy.

a. Available energy equations for hurricane volume. In this section, potential temperature is taken to be the vertical coordinate, since the available potential energy equations are exact in isentropic coordinates [Dutton and Johnson, 1967]. The total potential energy π of any region in hydrostatic balance is [Johnson, 1970]

$$\pi = \frac{C_p}{P_0^\kappa g(1 + \kappa)} \int_\sigma \int_0^\infty p^{1+\kappa} d\theta d\sigma \quad (42)$$

and that of the reference state π_r is

$$\pi_r = \frac{C_p}{P_0^\kappa g(1 + \kappa)} \int_\sigma \int_0^\infty p_r^{1+\kappa} d\theta d\sigma \quad (43)$$

The available potential energy A of the limited region ($\theta_0 \leq \theta \leq \theta_t$) equal to $\pi - \pi_r$ is then

$$A = \frac{C_p}{P_0^\kappa g(1 + \kappa)} \int_\sigma \int_{\theta_0}^{\theta_t} (p^{1+\kappa} - p_r^{1+\kappa}) d\theta d\sigma \quad (44)$$

where θ_0 is the coldest potential temperature in the region and θ_t is the isentropic surface above which the atmosphere is assumed to be barotropic. The θ_t surface may be considered coincident with the isobaric isothermal lid on the storm at height H . Since the pressure on isentropes that intersect the ground equals the surface pressure p_s , the available potential energy is

$$A = \frac{C_p}{P_0^\kappa g(1 + \kappa)} \left[\theta_0 \int_\sigma (p_s^{1+\kappa} - \langle p_s \rangle^{1+\kappa}) d\sigma + \int_\sigma \int_{\theta_0}^{\theta_t} (p^{1+\kappa} - \langle p \rangle^{1+\kappa}) d\theta d\sigma \right] \quad (45)$$

where the $\langle \rangle$ denotes an average over isentropic surfaces. In obtaining (45), we have used the conditions that for hydrostatic atmospheres, $p_r(\theta)$ equals $\langle p \rangle(\theta)$ and p_s equals $\langle p_s \rangle$.

If heating vanishes on the upper boundary, the time rate of change of A is [Johnson, 1970]

$$dA/dt = G(A) + C(A) + B(A) \quad (46)$$

where

$$G(A) = -\frac{1}{g} \int_\sigma \int_{\theta_0}^{\theta_t} [1 - \langle (p)/p \rangle^\kappa] \dot{Q} \frac{\partial p}{\partial \theta} d\theta d\sigma \quad (47)$$

$$C(A) = -\frac{1}{g} \int_\sigma \int_{\theta_0}^{\theta_t} (\mathbf{V} \cdot \nabla_\theta \psi) \frac{\partial p}{\partial \theta} d\theta d\sigma \quad (48)$$

$$B(A) = \frac{1}{g} \int_\sigma \int_{\theta_0}^{\theta_t} \nabla_\theta \cdot \frac{\partial p}{\partial \theta} (\psi - \psi_r) \mathbf{V} d\theta d\sigma \quad (49)$$

The generation $G(A)$ represents the effect of differential heating and is positive for heating at high pressure and cooling at low pressure on isentropic surfaces. The term $[1 - \langle (p)/p \rangle^\kappa]$ is frequently called the efficiency factor and is a measure of the effectiveness of heating or cooling in generating available energy. A vertical cross section through Hurricane Hilda (Figure 2) illustrates the mass-weighted efficiency factors for a mature hurricane. In this typical storm the pressures on the isentropes are highest at the center of the storm and decrease outward, so that heating (cooling) inside 600 km and cooling (heating) outside this radius contribute to a positive (negative) generation of available potential energy.

Although the largest positive efficiency factors are located in the eye, where latent heating is negligible, the efficiency factors are generally positive where the observed heavy rainfall and latent heat release occur. Therefore latent heating is effective in generating available energy. For this particular storm, Anthes and Johnson [1968] estimated generation by latent heat to be about 10×10^{12} W, a value that corresponds reasonably well to an estimate of 15×10^{12} W for kinetic energy production from mean hurricane data [Palmén and Riehl, 1957].

Although latent heating is the most important diabatic process in driving the storm, the cooling by infrared radiation in the clear environment surrounding the storm also contributes to a positive generation of available energy. Diabatic cooling rates are small ($\sim 2^\circ\text{C d}^{-1}$) in comparison to latent heating rates ($\sim 100^\circ\text{C d}^{-1}$); however, the greater area over which radiative cooling occurs results in a significant generation by this process for a domain of 1000-km radius or greater.

The conversion $C(A)$ of available potential energy to kinetic energy by cross-isobar flow provides the link between available potential energy and kinetic energy and was discussed in the preceding section.

In contrast to the small net boundary flux of kinetic energy the boundary term in the available potential energy equation may be quite large. The boundary term is written for cylindrical coordinates

$$B(A) = \frac{r_0}{g} \int_0^{2\pi} \int_{\theta_0}^{\theta_t} (\psi - \psi_r) u \frac{\partial p}{\partial \theta} d\theta d\lambda \quad (50)$$

We now consider the vertical correlation between $(u \partial p / \partial \theta)$ and $(\psi - \psi_r)$. The surface pressure on the θ_0 surface at the outer radius r_0 is greater than the mean pressure on θ_0 , which equals the mean surface pressure. Thus at the outer radius, $\psi < \psi_r$ in the low levels. In the upper troposphere, however, $\psi - \psi_r$ tends to vanish near the barotropic top of the storm. Since the radial motion is strongest at the surface ($u < 0$) and reverses sign in the upper troposphere, the covariance between $(u \partial p / \partial \theta)$ and $(\psi - \psi_r)$ is positive. Thus the integral

$B(A)$ provides a positive contribution to dA/dt . Physically, this term represents the transport of heat at high levels away from the storm system. Without this effective heat sink in the outer fringe of the storm the horizontal temperature gradient and associated baroclinity would be reduced as the air in the outer region subsided and warmed.

b. Energy balance in a steady state axisymmetric hurricane model. It is appropriate to summarize the discussion of hurricane energetics with an illustration of the balanced energy budget in a steady state model tropical cyclone [Anthes, 1971b]. The model is axisymmetric, and the horizontal and radial circulations are obtained as a function of applied thermal forcing. Figure 9 shows the evolution of the various components of the available potential energy and kinetic energy budgets as the model tropical cyclone approaches a slowly varying state.

In Figure 9 the conversion $C(A, K)$ of available to kinetic energy by cross-isobar flow of about 11.0×10^{12} W balances the sum of the dissipative effects of surface friction and internal mixing. This value is in good agreement with empirical energy budgets (section D2c). In turn, the available potential energy supply is maintained by the diabatic heating $G(A)$ and flow across the domain boundary $B(A)$, which is open at 500-km radius. As was noted previously, the net boundary flux of kinetic energy is small in comparison to the conversion and dissipation processes within the volume.

c. Empirical energy budgets. A number of kinetic energy budgets, summarized in Table 4, have been computed from hurricane data. In most of these studies the storm is assumed to be in a steady state, so that there is a balance between kinetic energy production, advection, and dissipation. Riehl and Malkus [1961], however, estimated the local time rate of change of kinetic energy and included this term in the balance.

The production of kinetic energy through cross-isobar flow and the advection of kinetic energy is estimated from observed wind data. The dissipation of kinetic energy at the sea surface is computed directly through the use of drag coefficients and the quadratic stress law. The dissipation of kinetic energy over the remainder of the storm outside the boundary layer is then estimated as a residual.

Most of the energy budgets shown in Table 4 were computed from aircraft data and therefore cover only the interior portion of the storm (100–150 km from the center). At these short distances from the center the advection of kinetic energy

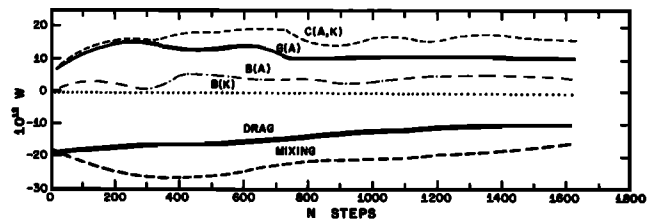


Fig. 9. Energy balance in slowly varying model of tropical cyclone [Anthes, 1971b]. Parameter $C(A, K)$ is the conversion of available to kinetic energy, $G(A)$ is the generation of available energy by latent heating, $B(A)$ is the change of available energy by horizontal flow across the lateral boundary, $B(K)$ is the net flux of kinetic energy across the lateral boundary, DRAG represents the loss of kinetic energy at the sea surface, and MIXING is the dissipation of kinetic energy by internal mixing.

from the outer portion of the storm is comparable to the production in the storm's interior. The sum of advection plus production should be comparable to the total production within the storm's domain ($r \leq 1000$ km). However, this estimate will be too small because part of the kinetic energy produced beyond this radius is also dissipated outside this radius and does not appear in the advection term.

The sum of kinetic energy production and advection for the 100–150 km inner region ranges from 3.05×10^{12} W for Hurricane Daisy on August 25 to 10.4 W for Hurricane Helene. The kinetic energy budget computed from the mean storm data indicates 15.0×10^{12} W over a domain of 666-km radius. Therefore for a mature hurricane a typical rate of kinetic energy production over a domain of 1000-km radius is about 15×10^{12} W.

The ratio of dissipation by internal friction to dissipation by surface friction varies over a wide range, from 0.17 for the mean storm to 2.1 for Hurricane Daisy on August 27. In view of this wide range the safest conclusion is that dissipation in the free atmosphere is of about the same order as boundary layer dissipation.

E. ANGULAR MOMENTUM CONSIDERATIONS IN THE TROPICAL CYCLONE

Preceding sections have related kinetic energy production to latent heating and shown that it is primarily the radial circulation that is involved in the important energy transformations. The production of the tangential circulation, which composes the greatest portion of the kinetic energy, has not

TABLE 4. Empirical Energy Budgets for Mature Hurricanes

Storm	Outer Radius of Domain, km	$\frac{\partial K}{\partial t}$	Components of Energy Budget, 10^{12} W				Available Potential Energy Generation (Latent Heating and Radiation)
			Advection	Production	Surface Dissipation	Internal Dissipation	
Hilda [Hawkins and Rubsam, 1968]	150	...	+3.9	+2.3	-4.2	-2.0	...
Hilda [Anthes and Johnson, 1968]	1000	10.3
Helene [Miller, 1962]	111	...	2.4	8.0	-5.1	-5.3	...
Daisy							
August 25	150	0.45	0.25	2.8	-1.6	-1.0	...
August 27	150	0.50	3.50	6.8	-3.2	-6.6	...
Riehl and Malkus [1961]							...
Mean storm [Palmén and Riehl, 1957]	666	...	0.00	15.0	-12.8	-2.2	...

been considered explicitly. In this section the conversion of radial to tangential momentum through the conservation of angular momentum is examined.

From an energetic viewpoint it is conceivable that the hurricane might exist in a steady state within a mechanically closed domain. In such a hypothetical system, latent and sensible heating near the hurricane center would be balanced by radiational loss in the outer regions, and kinetic energy production would be balanced by dissipation within the system. However, the amount of cyclonic angular momentum within a closed volume is limited, and loss of angular momentum is continuously occurring at the sea surface. A balanced angular momentum budget would require an annular region of substantial anticyclonic surface winds over the outer portion of the storm's domain. Observations [Miller, 1958] show cyclonic winds extending to great distances ($r > 900$ km) from the storm center; thus a steady state closed system is impossible on a scale of 1000 km. However, it is revealing to consider the angular momentum budget of the hurricane system and to estimate the influx of angular momentum required to maintain a steady state.

1. Development of Angular Momentum Budget Equations

We consider cylindrical coordinates with origin at the center of a stationary storm whose circulation vanishes at some upper level z_t . The tangential equation of motion may be written in terms of relative angular momentum $m = rv$:

$$\rho \frac{dm}{dt} = -r\rho fu - \frac{\partial p}{\partial \lambda} + r \frac{\partial \tau_{\lambda z}}{\partial z} \quad (51)$$

The total angular momentum M between concentric cylinders of radius r_0 and r_1 and levels z_0 and z_t is

$$M = \int_{z_0}^{z_t} \int_{r_0}^{r_1} \int_0^{2\pi} r \rho m \, d\lambda \, dr \, dz \quad (52)$$

The budget equation for the time rate of change of M in this limited region is obtained by use of the transport theorem

$$\begin{aligned} \frac{\partial M}{\partial t} = & \int_{z_0}^{z_t} \int_{r_0}^{r_1} \int_0^{2\pi} r \frac{dm}{dt} \, d\lambda \, dr \, dz \\ & - \int_0^{2\pi} \int_{z_0}^{z_t} [r_1(\rho mu)_{r_1} \\ & - r_0(\rho mu)_{r_0}] \, dz \, d\lambda \\ & - \int_0^{2\pi} \int_{r_0}^{r_1} r[(w\rho m)_{z_t} - (w\rho m)_{z_0}] \, dr \, d\lambda \quad (53) \end{aligned}$$

The combination of (51) and (53) and the fact that the tangential pressure gradient integrates to zero yield

$$\begin{aligned} \frac{\partial M}{\partial t} = & \int_{z_0}^{z_t} \int_{r_0}^{r_1} \int_0^{2\pi} \left(-r^2 \rho fu + r \frac{\partial \tau_{\lambda z}}{\partial z} \right) \, d\lambda \, dr \, dz \\ & - \int_0^{2\pi} \int_{z_0}^{z_t} [r_1(\rho mu)_{r_1} - r_0(\rho mu)_{r_0}] \, dz \, d\lambda \\ & - \int_0^{2\pi} \int_{r_0}^{r_1} r[(w\rho m)_{z_t} - (w\rho m)_{z_0}] \, dr \, d\lambda \quad (54) \end{aligned}$$

The integration to zero of the tangential pressure gradient shows that asymmetries in the pressure field, even if they exist, cannot change the circularly averaged angular momentum.

To illustrate the role of the Coriolis torque in the production of angular momentum, it is convenient to divide the

hurricane domain into two layers, a lower layer ($0 \leq z \leq h$), in which the azimuthally averaged radial velocity is inward, and an upper layer ($h \leq z \leq z_t$), in which the average radial velocity is outward. The level h may be considered the top of the boundary layer, where the inflow and tangential stress both vanish. The total angular momentum in each layer being denoted by M_1 and M_0 , respectively, the budget equation for the rate of change of M in each layer is

$$\begin{aligned} \frac{\partial M_1}{\partial t} = & - \int_0^h \int_{r_0}^{r_1} \int_0^{2\pi} (r^2 \rho fu) \, dr \, d\lambda \, dz \\ & - \int_{r_0}^{r_1} \int_0^\pi r^2 \tau_{\lambda z}(z=0) \, d\lambda \, dr \\ & - \int_0^{2\pi} \int_0^h [r_1(\rho mu)_{r_1} - r_0(\rho mu)_{r_0}] \, dz \, d\lambda \\ & - \int_0^{2\pi} \int_{r_0}^{r_1} r(w\rho m)_h \, dr \, d\lambda \quad (55) \end{aligned}$$

and

$$\begin{aligned} \frac{\partial M_0}{\partial t} = & - \int_h^{z_t} \int_{r_0}^{r_1} \int_0^{2\pi} (r^2 \rho fu) \, d\lambda \, dr \, dz \\ & - \int_0^{2\pi} \int_h^{z_t} [r_1(\rho mu)_{r_1} - r_0(\rho mu)_{r_0}] \, dz \, d\lambda \\ & + \int_0^{2\pi} \int_{r_0}^{r_1} r(w\rho m)_h \, dr \, d\lambda \quad (56) \end{aligned}$$

In obtaining (55) and (56) we have used the boundary conditions that vertical velocity vanishes at the surface and z_t and that the tangential stress is zero at h and z_t .

The relative importance of the circularly symmetric portion of the storm's circulation compared to the asymmetric portion of the flow may be studied by expanding the Coriolis term and the radial and vertical momentum flux terms as the sum of the circular mean and eddy component, neglecting horizontal density variations, and integrating over λ :

$$\begin{aligned} \frac{\partial M_1}{\partial t} = & -2\pi \int_0^h \int_{r_0}^{r_1} r^2 \rho(z) \langle (f')^\lambda \langle u \rangle^\lambda + \langle f'u' \rangle^\lambda \rangle \, dr \, dz \\ & - 2\pi \int_{r_0}^{r_1} r^2 \langle \tau_{\lambda z} \rangle^\lambda(z=0) \, dr - 2\pi \int_0^h r_1 \rho(z) \langle (m')^\lambda \langle u \rangle^\lambda \\ & + \langle m'u' \rangle^\lambda \rangle \, dz - 2\pi \int_{r_0}^{r_1} r \rho(h) \langle (w')^\lambda \langle m \rangle^\lambda \\ & + \langle w'm' \rangle^\lambda \rangle \, dr \quad (57) \end{aligned}$$

with a similar equation for $\partial M_0/\partial t$. The terms in (57), except for the $\langle f'u' \rangle^\lambda$ term, have been evaluated in angular momentum budgets for various regions of the hurricane domain by utilizing mean hurricane wind data by Pfeffer [1958] and Palmén and Riehl [1957]. Their results are presented in Table 5 for the outflow and inflow layers.

The first term in (57) is the Coriolis torque due to the mean radial motion and represents the conversion of radial to tangential circulation. The absence of the conversion term at the equator, where f equals zero, helps explain why tropical storm formation does not occur within 10° of the equator [Gray, 1967b]. As is shown in Table 5, the mean Coriolis torque represents a large positive contribution to the angular momentum budget in the inflow layer and the major negative contribution in the outflow layer. However, when the total

TABLE 5. Empirical Angular Momentum Budgets for Mature Hurricanes

Storm	Radial Domain, km	Coriolis Torque	Mean Horizontal Flux	Eddy Horizontal Flux	Mean Vertical Flux	Eddy Vertical Flux	Loss to Sea
<i>Lower Layer</i>							
Mean storm [Palmén and Riehl, 1957]	0-333	48.0	74.0	12.0	-40.0	-20.0	-74.0
	333-666	143.0	-9.0	26.0	...	-44.0	-116.0
Mean storm [Pfeffer, 1958]	222-444	54.0	22.0	8.0	-5.0	...	-8.5
	444-666	78.0	-1.0	26.0	4.0	...	-123.0
<i>Upper Layer</i>							
Mean storm [Palmén and Riehl, 1957]	0-333	-48.0	-20.0	8.0	40.0	20.0	
	333-666	-143.0	76.0	23.0	...	44.0	
Mean storm [Pfeffer, 1958]	222-444	-54.0	46.0	20.0	5.0	...	
	444-666	-78.0	-11.0	13.0*	-4.0	...	

Units are 10^{22} g cm² s⁻² unless they are specified otherwise.

* Pfeffer [1958] speculates that the large deficit in the upper layer from 444-666 km is due to underestimation of eddy flux by mean data.

depth of the storm's domain is considered, the net contribution by the Coriolis torque is very small because

$$\int_0^{z_1} \int_{r_0}^{r_1} \rho(z) \langle f \rangle \langle u \rangle dr dz = \langle f \rangle \int_{r_0}^{r_1} \int_0^{z_1} \rho(z) \langle u \rangle dz dr \quad (58)$$

and the vertically integrated radial mass flux is very nearly zero.

The eddy term $\langle f'u' \rangle^\lambda$ has been neglected in previous budget studies. For small radial domains, over which f is nearly constant, this term will be negligible. However, the contribution at larger radii may possibly be appreciable. At the 1000-km radius, for example, f varies by 46% of its mean value north of the center and 49% south of the center. If the inflow at this distance occurs asymmetrically with respect to the northern and southern semicircles, this term may not be negligible. Above-average inflow in the northern semicircle would produce a positive contribution to the angular momentum budget of the region.

The loss of angular momentum to the sea, represented by the third term in (57), is the only sink of angular momentum in the hurricane volume; the other terms represent transfers of angular momentum from one region to another. For a steady state storm inside a radial distance r_1 the angular momentum loss to the sea must be balanced by an inward flux across radius r_1 . An estimate of this required flux may be made by equating the radial flux in the layer $0 \leq z \leq h$ at r_1 to the total sink (S) of angular momentum inside this radius:

$$\langle uv \rangle^{\lambda z} = S/2\pi r_1^2 \rho^z h \quad (59)$$

where the $\langle \rangle^{\lambda z}$ denotes a tangential and vertical average. For ρ^z equal to 10^{-9} g cm⁻³, h equal to 1 km, r_1 equal to 666 km, and S equal to -190×10^{22} g cm² s⁻¹ from Palmén and Riehl's data (Table 5) we find $\langle uv \rangle^{\lambda z}$ equal to about 68 m² s⁻². This value represents a large mass exchange of the hurricane with its environment at this radius. For a symmetric inflow layer in which u and v are equal, the radial component would exceed 8 m s⁻¹. Thus the hurricane must be considered an open system at this radius.

2. Angular Momentum Distribution in the Hurricane

The absolute angular momentum per unit mass is defined by

$$m_a = m + (fr^2/2) \quad (60)$$

Because of the earth's contribution ($fr^2/2$), m_a normally in-

creases with increasing radius; i.e., the circularly averaged absolute vorticity is positive, since $\langle \zeta_a \rangle^\lambda = 1/r \partial \langle m_a \rangle^\lambda / \partial r$. Equation (51) may be written in terms of absolute angular momentum

$$\begin{aligned} \frac{dm_a}{dt} &= \frac{\partial m_a}{\partial t} + u \frac{\partial m_a}{\partial r} + \frac{v}{r} \frac{\partial m_a}{\partial \lambda} + w \frac{\partial m_a}{\partial z} \\ &= \frac{1}{\rho} \left(-\frac{\partial p}{\partial \lambda} + r \frac{\partial \tau_{r\lambda}}{\partial z} \right) \quad (61) \end{aligned}$$

A schematic vertical cross section of azimuthally averaged absolute angular momentum in a hurricane based on mean tangential wind data [Palmén and Riehl, 1957] is shown in Figure 10. In the inflow layer, $\langle m_a \rangle^\lambda$ increases with height because of surface friction. Inside the radius of maximum wind (R_0), where the horizontal shear is cyclonic, $1/r \partial \langle m_a \rangle^\lambda / \partial r$, which equals the absolute vorticity, is very large.

Outside R_0 , anticyclonic shear is present, and the absolute vorticity is much smaller. In the outflow layer, frictional torques are small, and the outflowing air tends to conserve its absolute angular momentum, so that $\partial \langle m_a \rangle^\lambda / \partial r \sim 0$. In the absence of friction, (61) indicates that steady state axisymmetric horizontal ($w = 0$) flow is possible in this region. However, the condition $\partial \langle m_a \rangle^\lambda / \partial r \sim 0$ requires that the tangential wind become more anticyclonic with increasing radius. Since the maximum anticyclonic wind speed is limited by the kinetic energy of the outflowing air, the $fr^2/2$ term dominates at larger radii, and $\partial \langle m_a \rangle^\lambda / \partial r$ becomes positive. This condition is represented in Figure 10 beyond the 500-km radius. Steady state axisymmetric flow in this outer region would require air to ascend into the stratosphere in order to conserve angular momentum. Such vertical motion in a region of high static stability requires extreme diabatic heating rates [Anthes, 1970]. Therefore steady state axisymmetric outflow is impossible at large distances ($r > 500$ km) from the storm center.

The outflow layer of actual storms indeed exhibits a great degree of asymmetry, as was indicated earlier by a sizable eddy flux of angular momentum. Fairly large scale eddies (wave numbers one and two around the storm) are persistent in time, and the transport of angular momentum by these eddies at radii greater than 500 km is sufficient to satisfy the above angular momentum and energy constraints [Palmén and Riehl, 1957; Pfeffer, 1958; Black and Anthes, 1971].

Because the angular momentum and energy constraints on the hurricane outflow have restricted the axisymmetric por-

tion of steady flow to $r < 500$ km, whereas the total angular momentum budget requires a large import of angular momentum across this radius to offset frictional loss to the sea, it follows that a closed steady state axisymmetric hurricane is impossible on any scale. A domain for which the axisymmetric assumption is valid ($r_0 \sim 500$ km) must be open at the lateral boundaries, and a net input of cyclonic relative angular momentum must occur to maintain the steady state. For domains on the order of 1000 km or greater the axisymmetric restriction is unrealistic.

F. WATER VAPOR BUDGET OF THE TROPICAL CYCLONE

The water vapor budget is extremely important in determining the intensity of the mature hurricane. A necessary condition for hurricane maintenance is the availability of an abundant water vapor supply in the Ekman boundary layer because water vapor convergence in this layer determines the latent heating rate. For a steady state storm the influx of moisture through the lateral boundaries plus evaporation from the sea must equal the precipitation. Because of the near equality between the two large terms representing diabatic heating and adiabatic cooling in the eye wall, hurricane intensity is very sensitive to small percentage changes in latent heating. Furthermore, the buoyancy of cumulus clouds is also sensitive to the surface equivalent potential temperature θ_e , which is a strong function of the low-level moisture content. In the eye wall, where lapse rates are nearly moist adiabatic, even a slight decrease in boundary layer θ_e will greatly reduce the buoyancy of cumulus clouds. Therefore evaporation is important not only in increasing the total amount of water vapor available for condensation but in maintaining a sufficiently large boundary layer θ_e so that cumulus convection may continue despite the increased static stability of the mature storm.

Although most meteorologists agree that evaporation from the sea surface represents a necessary process in maintaining a high boundary layer water vapor content, a recent alternative view regards the preexisting ambient water vapor in the hurricane environment as a sufficient source of boundary layer water vapor and minimizes the importance of evaporation [Carrier *et al.*, 1971]. This latter hypothesis will be examined in section G. At this point we derive a simplified water vapor budget and calculate the evaporation rate that is required to maintain a steady hurricane.

1. Water Vapor Budget Equations

Because of the decrease of temperature with height and the exponential decrease of saturation vapor pressure with

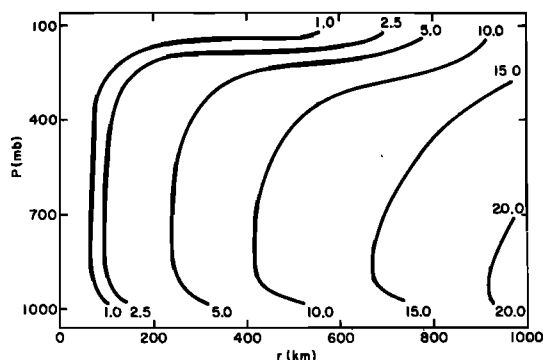


Fig. 10. Schematic cross section of absolute angular momentum in mature hurricane; units are 10^6 m^2/s .

temperature, atmospheric moisture decreases rapidly upward. This fact simplifies the water vapor budget, since most of the vapor in the ascending air in the eye wall condenses and falls out as rain. The outflow layer is too cold to contain significant amounts of water vapor, and very little vapor is returned into the lower portion of the storm system from the outflow layer.

The axisymmetric continuity equation for water vapor in pressure coordinates is

$$\frac{\partial q}{\partial t} + \frac{\partial q\omega}{\partial p} + \frac{\partial ruq}{r \partial r} = -P + E \quad (62)$$

where the storage of liquid water has been neglected for simplicity. The equations for the water vapor budget of a closed domain are derived by considering the subdivision of the hurricane domain shown in Figure 8. In the water vapor budget the radius R_0 of Figure 8 should be considered the radius separating mean upward motion (boundary layer convergence) from mean downward motion (boundary layer divergence) and is about 300 km.

In this simplified system, boundary layer moisture (region II) is supplied by evaporation from the sea, weak subsidence from region I, and, in an open system, horizontal flux across radius r_0 . Region II supplies water vapor to region III by inward flow across radius R_0 . Most of this vapor condenses and falls out as precipitation as the air rises in region III, only a small amount of vapor, liquid water, and ice crystals being left for export into region IV. The problem is to estimate quantitatively the components of the water vapor budget in a steady state hurricane given the radial and vertical mass circulation.

In the budgets discussed in this paper we consider radially uniform subsidence beyond R_0 and vertically constant radial flow in the boundary layer (region II). These assumptions are equivalent to the neglect of horizontal and vertical eddy fluxes of water vapor between regions.

To reduce the specification of the radial and vertical mass circulation to a single parameter U , the mean inflow in the boundary layer across radius R_0 , we note that the mass inflow (ru) is relatively constant with radius in hurricanes [Malkus and Riehl, 1960]. Thus specification of U and R_0 tends to represent the mass inflow over the entire domain. If $R_0 U$ is specified and ω is assumed to be independent of r beyond R_0 , integration of the continuity equation yields

$$\omega_1 = \frac{2[r_0 u(r_0) - R_0 U]}{(r_0^2 - R_0^2)} (p_0 - p_1) \quad (63)$$

where ω_1 is the vertical velocity at the top of the boundary layer in region II. Beyond R_0 , where low-level divergence of water vapor exists, cumulus convection is suppressed. Therefore precipitation may be neglected. If Q_{II} is defined as the average boundary layer value of (rq) ,

$$Q_{II} \equiv \langle rq \rangle^{rp} = (r_0 - R_0)^{-1} (p_0 - p_1)^{-1} \cdot \int_{p_1}^{p_0} \int_{R_0}^{r_0} (rq) dr dp \quad (64)$$

where p_0 is the surface pressure and p_1 is the pressure at the top of the boundary layer, and (62) is integrated over region II, the time-dependent equation for water vapor in the boundary layer is

$$\frac{dQ_{II}}{dt} = \frac{-\langle \omega_1 \rangle^r \langle rq_1 \rangle^r}{p_0 - p_1} + \frac{UR_0 \langle q(R_0) \rangle^p}{r_0 - R_0} + \langle rE \rangle^{rp} \quad (65)$$

In region I the only term in the continuity equation is the sink of air subsiding into the boundary layer,

$$\frac{dQ_I}{dt} = -\frac{\omega_1}{(p_1 - p_2)} \langle r q_1 \rangle^r \quad (66)$$

where Q_I is the average value of (rq) in region I. The net precipitation and evaporation in region III may be estimated from the inflow into region III:

$$P - E = -\frac{(p_0 - p_1)}{\pi R_0 g} \langle U q(R_0) \rangle^p \quad \text{cm rain s}^{-1} \quad (67)$$

The solutions to (65) and (66) are easily obtained as a function of U and R_0 once values of (rq) at the interface of each region are related to the average values over each region. We note that $q(R_0) \approx q(r)$ in the inflow layer, which yields

$$\langle R_0 q(R_0) \rangle^p = \frac{2R_0(r_0 - R_0)}{(r_0^2 - R_0^2)} Q_{II} \quad (68)$$

To obtain q_1 as a function of the mean specific humidity in the middle-tropospheric region between pressures p_1 and p_2 , we note that observations show an exponential decrease of q with pressure and assume

$$q(p) = q_1 e^{\lambda(p_1 - p)} \quad (69)$$

where λ equals $(p_1 - p_2)^{-1} \ln(q_2/q_1)$. From (69) the average specific humidity in the layer between p_1 and p_2 is

$$\langle q \rangle^p = -\frac{q_1}{\lambda(p_1 - p_2)} (1 - e^{\lambda(p_1 - p_2)}) \quad (70)$$

which determines q_1 as a function of the average humidity in the layer:

$$q_1 = -\frac{\ln(q_2/q_1)}{(1 - q_2/q_1)} \langle q \rangle^p \quad (71)$$

Substituting (68) and (71) into (65) and (66), we find

$$\frac{dQ_{II}}{dt} = \beta_0 Q_I + \beta_1 Q_{II} + S \quad (72)$$

$$\frac{dQ_I}{dt} = -\frac{(p_0 - p_1)}{(p_1 - p_2)} \beta_0 Q_I$$

where

$$\beta_0 = \frac{\omega_1}{(p_0 - p_1)} \frac{\ln(q_2/q_1)}{(1 - q_2/q_1)} \quad (73)$$

$$\beta_1 = \frac{2R_0 U}{(r_0^2 - R_0^2)} \quad (74)$$

$$S = \langle rE \rangle^r \quad (75)$$

The solutions to (72) are

$$Q_I(t) = Q_I(t_0) \exp\left(-\frac{p_0 - p_1}{p_1 - p_2} \beta_0 t\right) \quad (76)$$

and

$$Q_{II}(t) = Q_{II}(t_0) e^{\beta_1 t} - \left\{ \beta_0 Q_I(t_0) \left[\exp\left(\frac{p_0 - p_1}{p_1 - p_2} \beta_0 t\right) - \exp(\beta_0 t) \right] \right\} \left(\frac{p_0 - p_1}{p_1 - p_2} \beta_0 + \beta_1 \right)^{-1} - \frac{S(e^{\beta_1 t} - 1)}{\beta_1} \quad (77)$$

The survival time of a storm based only on the availability of preexisting water vapor in the hurricane domain may be estimated by evaluating (77) for a closed domain in which evaporation (S) is zero. Initial conditions are $\langle q \rangle^p$ in the boundary layer, q_1 equal to 20 g kg^{-1} , and q_2 equal to 2 g kg^{-1} . The specific humidity in the boundary layer after 10 days is shown in Figure 11 as a function of domain size (r_0) and inflow (U) across R_0 , which is a measure of storm intensity. Without evaporation a domain of at least 2000-km radius is necessary to maintain a nearly constant boundary layer humidity for 10 days. Thus either evaporation or horizontal advection of moisture is essential for a steady state moist boundary layer. We next determine whether the required magnitude of evaporation is possible, and what size domain is required for evaporation to equal precipitation.

On the basis of turbulence theory [Jacobs, 1951; Sverdrup, 1951] the latent heat flux from the sea surface (F_L) is proportional to the wind speed and the difference between the saturation specific humidity at the sea surface temperature and the specific humidity of the air:

$$F_L = \rho C_E |\mathbf{V}| (q_{\text{sea}} - q) \quad q_{\text{sea}} \geq q \quad (78)$$

where C_E is an empirically determined exchange coefficient and F_L is expressed in grams of water vapor per square centimeter per second. The rate of addition of water vapor in the boundary layer of depth h is then

$$E = -\frac{1}{\rho} \frac{\partial F_L}{\partial z} = \frac{C_E |\mathbf{V}| (q_{\text{sea}} - q)}{h} \quad (79)$$

It is noteworthy that the assumptions made in the derivation of (78) are best satisfied under conditions of strong winds and that the flux predicted by this formula is most accurate when the transfer is large [Garstang, 1967].

To determine the size of the domain for which evaporation could equal precipitation, we consider the extreme case in which advection of moisture from the middle troposphere is neglected and set

$$\langle rE \rangle^r = \frac{\langle C_E |\mathbf{V}| (q_{\text{sea}} - q)r \rangle^r}{h} = -\frac{R_0 U q(R_0)}{(r_0 - R_0)} \quad (80)$$

If the covariance between $C_E |\mathbf{V}| (q_{\text{sea}} - q)$ and r is ignored, a rough estimate of the radius of the domain for which evaporation equals precipitation inside r_0 is

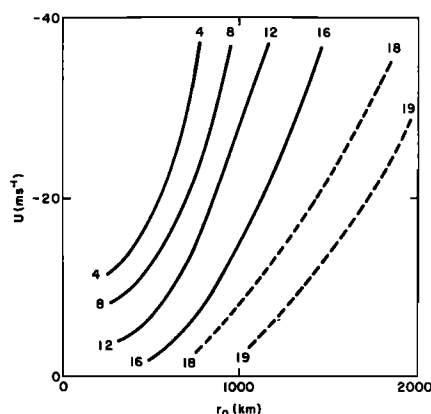


Fig. 11. Mean boundary layer specific humidity (grams per kilogram) after 10 days under steady state radial circulation in a closed domain. Initial specific humidity is 20 g/kg .

$$r_0 = \left(R_0^2 + \frac{2hUR_0q(R_0)}{C_E(q_{\text{sea}} - q)|V|^r} \right)^{1/2} \quad (81)$$

The exchange coefficient C_E for trade wind conditions is approximately 2×10^{-3} [Riehl *et al.*, 1951; Garstang, 1967]. Malkus and Riehl [1960] showed that C_E had about the same value in hurricanes. They note, however, that the actual exchange of latent heat is larger in hurricanes because of the dependence of F_L on wind speed. To estimate $(q_{\text{sea}} - q)$, we assume a mean sea-air temperature difference of 1°C , which yields a $(q_{\text{sea}} - q)$ of $1.5 \times 10^{-3} \text{ g g}^{-1}$ for temperatures about 27°C . The remaining parameters are assigned the following values: $R_0 = 300 \text{ km}$, $h = 1 \text{ km}$, $U = 10 \text{ m s}^{-1}$, and $|V| = 10 \text{ m s}^{-1}$. For these estimates the value of r_0 computed from (81) is about 1700 km. Thus evaporation over a domain size of the order of 2000-km radius could easily replenish the boundary layer moisture supply. In the more general case in which the downward flux of moisture from the middle troposphere is considered, the required evaporation would be less.

In a steady system, in which there is no net lateral inflow of water vapor, the ratio of evaporation to precipitation will approach unity as the ambient reservoir of moisture is depleted. Figure 12 shows the required ratio of evaporation to precipitation in a steady state closed system after 10 days (obtained from equations (71) and (72)). Even for weak storms of large radial extent the evaporation represents a significant contribution to the water vapor budget.

In summary, the water vapor budget for a closed system indicates that evaporation from the sea must equal a significant percentage of the precipitation rate in order to maintain a steady hurricane. Furthermore, the required evaporation rate is easily obtained over domains of 1500- to 2000-km radius.

2. Empirical Water Vapor Budgets

In the previous section the water vapor budget for the entire hurricane system was discussed for a domain with radius of the order of 1000–2000 km. Empirical budgets for domains of this size are not available; however, a number of budgets for much smaller domains ($r \sim 150 \text{ km}$) have been reported (Table 6).

In the water vapor budgets presented in Table 6 the inward horizontal transport of water vapor from the outer portion of the storm dominates the evaporation inside the 150-km radius, since the inflow is very strong at this distance and the sea surface area inside this radius is relatively small. Nevertheless, evaporation is a significant source of water vapor, varying between 12 and 54% of the horizontal transport.

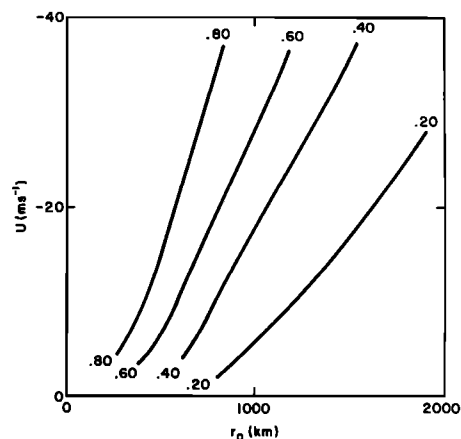


Fig. 12. Ratio of evaporation to precipitation required to maintain a boundary layer of constant water vapor supply after 10 days in a closed system.

Also included in Table 6 are two estimates of evaporation over radial rings of relatively small areas near the center of Hurricane Betsy [Machta, 1969]. These direct estimates are made from Ostlund's [1967] tritium measurements and are comparable to the indirect estimates made by previous investigators.

As the outer radius of the hurricane volume increases, the ratio of evaporation within the volume to transport across the boundary undoubtedly increases. Beyond about 500 km, where the mean radial mass flux decreases with increasing radius, the evaporation may become the dominant source of water vapor to the entire volume.

G. MODELING OF TROPICAL CYCLONES

The preceding sections have discussed the physics of mature tropical cyclones and the constraints upon the hurricane system that are imposed by the energy, angular momentum, and water vapor budgets. Although such a simplified treatment is instructive in understanding the hurricane, it is of little practical use in predicting individual storms. In order to forecast hurricane development and motion successfully with actual data, the equations describing the behavior of the atmosphere must be solved, or approximately solved, in a manner that retains all the significant physical processes discussed in the earlier sections. Second-order effects that are neglected in scaling estimates must also be retained. Certainly, the simplifying assumptions of axisymmetry and steady flow must be abandoned. Faced with the complexity of the time-dependent equations in three

TABLE 6. Empirical Water Vapor Budgets for Mature Hurricanes

Storm	Radial Ring, km	Horizontal Transport, 10^9 g s^{-1}	Evaporation, 10^9 g s^{-1}	Evaporation/Horizontal Transport, %
Hilda [Hawkins and Rubsam, 1968]	0–150	62.4	33.6	54
Helene [Miller, 1962]	0–111	132.6	21.8	16
Daisy				
August 25	0–150	70.0	12.6	18
August 27 [Palmén and Riehl, 1957]	0–150	164.0	19.7	12
Betsy (from tritium measurements [Machta, 1969] September 3, 1965)	91–128	...	17.4	...
September 5, 1965	73–165	...	23.2	...

spatial dimensions, meteorologists have turned to the computer in an effort to progress beyond the qualitative understanding of hurricane dynamics and energetics.

With the sudden increase in computer capability and availability in the 1960's, progress in tropical cyclone modeling has been spectacular. Numerical simulations of symmetric and asymmetric hurricanes have contributed to the understanding of the dynamics and energetics of these storms. However, the numerical prediction of hurricane development and motion with observational data has essentially been postponed in deference to basic theoretical modeling. Much more work is needed on the development of models that will be useful to the forecaster who must predict the behavior of individual storms.

This section reviews several recent tropical cyclone models, which are listed in Table 7. Although this section is primarily concerned with time-dependent models, one steady state analytic model is discussed briefly.

1. Carrier's Steady State Hurricane Model

An analytic approach to the steady state axisymmetric hurricane problem has recently been proposed by *Carrier et al.* [1971] in an interesting and thought-provoking analysis of hurricane dynamics. Carrier partitioned the hurricane into

four dynamically distinct regions: an updraft region of intense convection that tilts outward with height and includes the outflow layer, a boundary layer, an inactive region separating the outflow and inflow layers, and the eye, in which subsidence of dry air occurs. Approximate solutions for the axisymmetric quasi-steady hurricane were obtained analytically for these four regions. A major advantage of the Carrier model compared to the numerical models is its simplicity, since the essential features of hurricane dynamics may be described without resort to extensive computing facilities.

The basic physics of Carrier's model is very similar to that of other models. Latent heating is the primary energy source. Subsidence of dry warm air in the eye produces the extremely low pressures observed in hurricanes. The inflow circulation is produced when surface friction destroys the gradient balance between Coriolis, centripetal, and pressure gradient forces. The tangential circulation develops in the inflow layer through the conservation of angular momentum.

A difference between Carrier's analytic model and numerical models is that he emphasizes the environmental reservoir of moisture supply necessary to drive the storm. The numerical models indicate that hurricane maintenance is strongly dependent on increased evaporation from the sea. In Carrier's view the water vapor supply is the ambient energy

TABLE 7. Summary of Numerical Models of the Tropical Cyclone

Investigator	Model Type	Horizontal Dimensions	Vertical Layers	Latent Heating Type	Remarks
<i>Ogura</i> [1964]	prognostic balanced	1	2	Cu parameterization	The large-scale circulation showed slow development, but the growth of the meridional circulation was unbounded.
<i>Ooyama</i> [1964, 1967, 1969]	prognostic balanced	1	3	Cu parameterization	Evolution and structure of model hurricane compared favorably with storms in nature.
<i>Kuo</i> [1965]	prognostic balanced	1	2	Cu parameterization	Steady solutions were obtained in experiments without a separate boundary layer; unbounded growth occurred in experiments that included an explicit boundary layer.
<i>Yamasaki</i> [1968a, b]	prognostic P. E.†	1	4* 13‡	Cu parameterization	Multilevel model experiments investigated the importance of surface humidity, vertical partitioning of latent heat, and initial static stability.
<i>Miller</i> [1969]	prognostic P. E.†	2 (coarse mesh)	6	Cu parameterization and pseudoadiabatic	Forecasts utilized real data. The development of a large hurricane was forecast.
<i>Rosenthal</i> [1969, 1970a, b, 1971a, b]	prognostic P. E.†	1	6	Cu parameterization	Multilevel model utilized to study radial resolution. An explicit water vapor cycle was added [<i>Rosenthal</i> , 1970b], and nonconvective latent heat release modeled. The effect of initial humidity was studied. Artificial enhancement of heating was investigated [<i>Rosenthal</i> , 1971a].
<i>Sundqvist</i> [1970a, b]	prognostic balanced	1	10	Cu parameterization	The vertical partitioning of latent heat release, radiational cooling, and artificial enhancement of heating were investigated.
<i>Anthes</i> [1971a]	prognostic P. E.†	1	3	Cu parameterization	The effect of artificial redistribution of latent heating on storm intensity was investigated.
<i>Anthes et al.</i> [1971a, b]	prognostic P. E.†	2	3	Cu parameterization	Asymmetric model results [<i>Anthes et al.</i> , 1971a] were compared with axisymmetric results [<i>Anthes et al.</i> , 1971b]. Spiral bands and an asymmetric outflow layer were present in the model storm.
<i>Carrier et al.</i> [1971]	steady state	1	...	pseudoadiabatic	Analytic solutions to approximate steady state equations of motion were obtained over four separate regions of hurricane domain.

* For data by *Yamasaki* [1968a].

† P. E. denotes primitive equation model.

‡ For data by *Yamasaki* [1968b].

profile of the hurricane environment, which is maintained by 'sensible and latent heat from the warm sea surface, by vertical diffusion (in which we include cumulus convection) and by radiative loss to space.' According to Carrier these processes maintain the moisture content of the middle tropopause against the drying and warming effects of environmental subsidence.

A difficulty with Carrier's theory lies in the reliance upon cumulus convection to maintain the necessary high environmental moisture content. Observations indicate that deep widespread cumulus convection over the ocean occurs only in regions of low-level convergence [Malkus and Riehl, 1964]. This observation is the basis of cumulus parameterization theories [Kuo, 1965; Charney and Eliassen, 1964], which restrict significant cumulus convection to regions of low-level moisture convergence. In the outer environment of a hurricane, frictionally induced low-level divergence effectively prohibits tall cumulus convection. In fact, one of the earliest recognized signs of an approaching storm is the unusual suppression of normal tropical cloudiness, and satellite pictures confirm that the hurricane environment is relatively cloud free. Therefore the air that subsides into the boundary layer may be quite warm, but it is unusually dry and increased evaporation is necessary to replenish the moisture content.

It is noteworthy that the time-dependent models have evaluated the possibility that the mature storm may survive for a significant period of time on the preexisting tropospheric water vapor supply by reducing evaporation from the sea or eliminating the evaporation altogether. Experiments of this nature with models that are quite different in their numerical formulation [Ooyama, 1969; Rosenthal, 1971b] provide strong evidence that increased evaporation is essential in the maintenance of the hurricane. These models demonstrate that storm intensity is very sensitive to small reductions in boundary layer water vapor and hurricanes are unable to survive more than a few hours on the existing water vapor supply.

Although the axisymmetric steady models are useful in studying particular processes in a mature hurricane, they are by nature incapable of describing the complicated interactions and feedbacks between all the variables that are responsible for the growing, mature, and decaying stages of the tropical storm. To treat these interesting interactions fully and obtain solutions of practical use to the forecaster, a complete time-dependent model is necessary.

2. Prognostic Models

Early numerical experiments with prognostic multilevel axisymmetric models were able to continue for only several hours before growth of the smallest resolvable scale associated with gravitational instability dominated the calculations. The unbounded growth of the small convective scale in preference to the cyclone scale was a consequence of the appropriateness of the latent heating formulation to the cloud scale rather than the hurricane scale. In extratropical regions, which are normally conditionally stable, most of the large-scale condensation heating is derived from stable moist adiabatic ascent. In the conditionally unstable tropics, however, large-scale lifting results in small-scale convection [Bjerknes, 1938]. The large-scale heating of the environment by these smaller-scale clouds is a complicated process involving entrainment, horizontal and vertical mixing, and vertical eddies on the cloud scale, including compensating downdrafts, as was shown by Gray [1972] and Yanai *et al.* [1973]. The early model experiments with the pseudoadiabatic type of

large-scale heating showed that the hurricane was not a simple system composed of uniform pseudoadiabatic ascent of moist air. The difficulty with incorporating the latent heating process in a hurricane model was recognized by Syono [1962], who suggested that the convective scale should be treated separately from the cyclone scale.

a. Conditional instability of the second kind. In an effort to explain the growth of the hurricane scale disturbance in a conditionally unstable atmosphere. Charney and Eliassen [1964] and Ooyama [1964] proposed that the cumulus scale and the tropical cyclone scale disturbances cooperate rather than compete in the cyclone system, the convection providing the release of energy needed to drive the storm and the large-scale frictionally induced convergence of moisture providing the fuel for the convection. Growth of the larger-scale quasi-balanced circulation due to this interaction, termed 'conditional instability of the second kind (CISK),' occurred on reasonable time and space scales for the developing tropical depression. The CISK concept circumvented the problem of the explicit prediction of convective heat release and the associated gravitational instability and provided for a rapid advance in hurricane modeling.

An early and simple scheme for parameterizing the release of latent heat and vertical transport of water vapor was proposed by Kuo [1965]. An essential feature of the Kuo-type parameterization is the integral constraint imposed on the total amount of convective heat release in a column by the large-scale convergence of moisture. Because of the rapid decrease of water vapor with height and the strong frictional convergence in the low levels the total moisture convergence may be approximated by the vertical flux of moisture through the top of the Ekman boundary layer. In a conditionally unstable atmosphere the Kuo-type parameterization may be represented by

$$\dot{Q}(z) = \delta L W(z) I \left(\int_0^\infty W(z) dz \right)^{-1} \quad (82)$$

where \dot{Q} is the rate of heat addition per unit mass, I is the vertically integrated moisture convergence

$$I = \int_0^\infty \frac{\partial q}{\partial t} dz$$

$W(z)$ is a parameter specifying the vertical distribution of the total heating, and δ is a parameter that is 1 if I is positive and zero otherwise. In the above parameterization the heating at a particular level is not proportional to the vertical velocity at that level as it is in the case of stable moist adiabatic ascent. The difficulty with the Kuo-type parameterization is that the physical mechanisms governing the weighting function $W(z)$ are poorly understood, so that the use of (82) in hurricane models remains a pragmatic solution to the different interaction problem.

The parameterization of cumulus convection was first incorporated into axisymmetric models by Ogura [1964] and Kuo [1965] and was later used by Yamasaki [1968a, b], Rosenthal [1969, 1970a, b], Sundqvist [1970a, b], and Anthes *et al.* [1971a, b]. Ogura's vertically truncated model required only the total heat release in a column; the vertical distribution in Kuo's model was specified through a weighting function that depended on the thermodynamic properties of the cloud and the environment.

The use of the cumulus parameterization in Ogura's and Kuo's models eliminated the rapid growth of the convective

scale motions. However, the constant static stability in Ogura's model prevented a stabilization by the upward heat transport, so that unrealistic growth occurred. Furthermore, as was noted by Ogura and Kuo, the inexact formulation of the vertical velocity at the top of the boundary layer (which governs the total convective heating) contained the absolute vorticity in the denominator. Therefore the vertical velocity became unbounded as the absolute vorticity in the anticyclonic shear beyond the radius of maximum wind tended toward zero.

b. Recent axisymmetric hurricane models. Ooyama [1964, 1967, 1969] modeled the tropical cyclone with an energetically consistent balanced three-layer model of an incompressible homogeneous fluid. Ooyama's model was the first to exhibit a life cycle of growth, maturity, and decay. The structure and energy budget associated with his model were remarkably similar to those of hurricanes. Several experiments demonstrated the importance of a high sea surface temperature and the related sensible and latent heat supply from the ocean, a result confirmed by later models [Rosenthal, 1971*b*]. Variations in the drag coefficient and the coefficient of latent and sensible heat exchange were found to be crucial parameters in determining the development of the model storm. It was also shown that the rate of development, but not the ultimate structure of the mature storm, was dependent on the strength of the initial vortex.

Further aspects of the hurricane were studied with axisymmetric multilevel models by Yamasaki [1968*a, b*] and Rosenthal [1969, 1970*a, b*; 1971*a, b*]. Both of these models utilized primitive equations rather than balanced equations and formulated the latent heating parameterization following Kuo's theory. Yamasaki [1968*a, b*] studied the vertical partitioning of the latent heat and the effect of variations in the initial static stability, water vapor content of the surface air, Coriolis parameter, and drag coefficient. He found increasing horizontal scale with increasing latitude, more rapid development with a larger proportion of heat released in the middle rather than upper troposphere, and an increasing rate of development with increased surface humidity and drag coefficient.

Rosenthal's [1970*a*] seven-level model showed that a 10-km horizontal grid gave a significantly more realistic model hurricane structure than a 20-km grid. In particular, a well-defined persistent eye was present in the 10-km experiments but was only a poorly defined transient feature in the 20-km experiments.

The absence of an explicit large-scale water vapor cycle was a deficiency present in the above hurricane models. In the first experiments, which contained an explicit forecast of water vapor, Rosenthal [1970*b*] found that the initial large-scale relative humidity was an important variable in determining the development rate of the hurricane. In agreement with observations, nonconvective precipitation was a significant percentage of the total rainfall. His model also provided for the possibility of convection originating from layers other than the boundary layer if conditional instability and a supply of water vapor were present simultaneously. Further experiments with this model [Rosenthal, 1971*b*] showed that the addition of latent heat at the sea-air interface was far more important than the addition of sensible heat.

Sundqvist's [1970*a*] ten-level axisymmetric model verified Yamasaki's [1968*a*] finding that more rapid storm development occurred when a larger proportion of heat was released

in the middle troposphere. He later found that radiative cooling increased the rate of development but did not significantly affect the maximum intensity of the storm [Sundqvist, 1970*b*].

c. Utilization of axisymmetric models to simulate storm modification. Although hurricane modification simulation experiments are currently a subject of controversy, the immense importance of the subject warrants a brief review. The testing of hypotheses for hurricane modification is an important potential use for hurricane models. Two approaches to the hurricane modification problem that have received considerable attention are the suppression of evaporation from the sea and the seeding of cumulus clouds within the hurricane. The probable effect of the reduction of evaporation is relatively certain from a theoretical viewpoint. As was indicated earlier, model storm intensities are strongly dependent on evaporation from the sea. However, the technological difficulties of suppressing evaporation under hurricane conditions have prevented experimentation along these lines.

Although the probable effect of cloud seeding on hurricane intensity is far more obscure than that of a reduction in evaporation, cloud-seeding technology is relatively advanced, and hurricane modification by this technique has been attempted on several occasions [Gentry, 1969, 1970]. The determination of the response of the hurricane to cloud seeding is very complicated. We must determine not only the response of the individual clouds to the seeding but also the subsequent feedbacks between the cloud and the hurricane scale motions.

Several variations of the cloud-seeding hypothesis are discussed by Gentry [1969] and Rosenthal [1971*a*]. The most promising hypothesis of maximum wind reduction is based on the increase of cumulus convection at some distance beyond the outer edge of the main ring of convection (the eye wall). This increased convection at a greater radius from the storm center would compete with the old eye wall for the available water vapor and angular momentum in the inflow layer. If the percentage of total inflowing air that reaches the small radial distance of the old eye wall decreases, angular momentum considerations require a reduction in maximum wind speed.

Although the parameterization of cumulus convection in the numerical models has been very crude, several axisymmetric models have been utilized as guidance for field modification experiments that involve cloud seeding in hurricanes. However, hurricane models do not yet contain an explicit treatment of cloud physics appropriate to cumulus convection. The models that employ cumulus parameterizations can simulate only the effect of an artificial increase in the latent heating function on the storm's dynamics. These models assume that cloud seeding results in an increase in the transfer of heat to the large scale. Results from these experiments have been somewhat ambiguous, mainly because of the variations in the models and in the numerical treatment of the seeding effect.

Rosenthal [1971*a*] and Rosenthal and Moss [1971] showed that adding heat beyond the radius of maximum wind was more effective in reducing maximum wind speed than adding heat inside the radius of maximum wind. Sundqvist [1970*b*] found that a heating increase by a factor of 2 or 3 at large radii had the desired qualitative effect of spreading out the maximum vertical motion but that the magnitude of the maximum wind reduction was very small, a result later supported by Anthes [1971*c*]. Anthes [1971*a*] obtained reductions in maximum wind speed by as much as 50% with relatively small

redistributions in the latent energy of the storm; however, the amount of reduction depended greatly on the arbitrary form of the redistribution.

On the other hand, *Sundqvist* [1972] found an increase of maximum wind speed associated with a heating increase, regardless of where the heating was applied. He found the greatest increase when the heat was added inside the radius of maximum wind. The increase when heat was added beyond the radius of maximum wind was apparently due to increased water vapor convergence at all radii caused by the artificial heating.

We may conclude that the models have been of some use in testing various seeding hypotheses but have not yet provided conclusive answers regarding the effect of seeding on hurricane intensity. Models now being developed [*Rosenthal*, 1973] in which the cumulus convection is treated more realistically will be useful in assessing the effect of cloud seeding.

3. A Three-Dimensional Hurricane Model

Although several of the axisymmetric models have given results that correspond to a typical or mean hurricane, it is well recognized that a complete understanding of the hurricane and its interaction with the environment necessitates consideration of the full three-dimensional structure. Computer and economic restrictions have, until recently, restricted the development of a three-dimensional model. *Miller's* [1969] three-dimensional tropical forecast model predicted tropical storm development from a wave disturbance; however, his coarse horizontal mesh of 140 km precluded study of the hurricane scale dynamics.

Anthes et al. [1971a] studied the life cycle of the asymmetric tropical cyclone by utilizing a three-layer model with a 30-km horizontal grid. Despite the coarse horizontal and vertical resolutions the model reproduced many observed features of the three-dimensional tropical cyclone, including spiral rainbands and a strongly asymmetric outflow layer. Comparison of the three-dimensional model with a two-dimensional analog [*Anthes et al.*, 1971b] showed little difference between the circularly averaged asymmetric storm and the symmetric model storm, a result that supported previous results utilizing axisymmetric models.

Later experiments with a more advanced version of the asymmetric model [*Anthes*, 1972] established that a form of dynamic instability of the horizontal flow in the outflow layer was the primary cause of the development of asymmetries, the kinetic energy of the azimuthal mean flow providing the energy for the eddies. Rapid growth of the asymmetries in the outflow layer was associated with the production of negative absolute vorticity.

Well-defined and persistent rainbands occurred in the later version of the model (Figure 13). The formation of these bands was nearly simultaneous with the breakdown of symmetry in the upper-level flow, a coincidence that suggested a possible relation between the two events. The spiral bands formed continuously near the center of the storm and propagated outward at a speed of about 12 m s^{-1} .

4. Summary of Model Results

Besides the obvious achievement of proving that hurricanes can be simulated by numerical methods several important contributions to our knowledge of hurricane dynamics have emerged from the model experiments during the past decade. Many of these were quantitative confirmations of ideas and

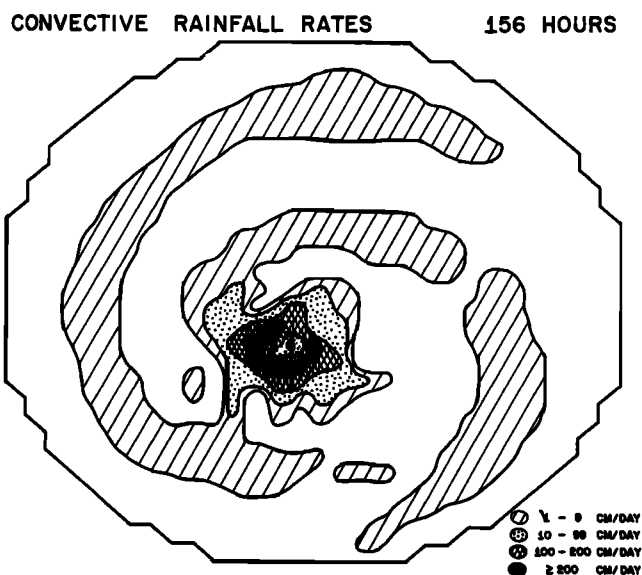


Fig. 13. Vertically integrated convective heat release expressed as rainfall rates (centimeters per day) in a time-dependent three-dimensional hurricane model [*Anthes*, 1972].

results painfully deduced over the years from meager hurricane data. The main conclusions and results are:

1. The realistic results from symmetric models show that the essential ingredients of tropical storm formation and maintenance may be described by azimuthally invariant processes, at least for relatively small distances from the storm center.
2. The model results indicate that hurricane formation and maintenance are critically dependent on sensible, and especially latent, heat addition from the sea. Model storms are very sensitive to variations in boundary layer water vapor content.
3. The models exhibit great sensitivity to relatively small variations in sea surface temperature. (This result may be viewed as a corollary to the second result.) A drop of 1° or 2°C may reduce maximum winds by 50% or more.
4. The development of model hurricanes is quite sensitive to the initial kinetic energy of the disturbance and to the initial large-scale static stability and moisture distribution, in addition to the sea temperature. For attainment of hurricane strength in a reasonable time (1–5 days) the moisture and temperature structure of the environment in the vicinity of a cyclonic disturbance must be unusually favorable for intensification; thus hurricane development is relatively infrequent.
5. The overall size of the storm, as predicted by linear theory, is a function of latitude, larger storms occurring at higher latitudes.
6. The development of horizontal asymmetries in the outflow layer appears to be related to dynamic instability, mean kinetic energy being converted to eddy kinetic energy through barotropic processes. The dynamic instability is not necessary for the formation of tropical cyclones but may be generated as a consequence of overall storm development.
7. Model hurricanes indicate that some reduction in maximum wind speed near the center might follow from an increase of heating at distances beyond the radius of maximum wind. This result is tentative and will require confirmation

with models in which the cloud seeding is more accurately treated.

In the next decade we may anticipate much more work with fully three-dimensional hurricane models and the consideration of storm movement and interaction with the environment. More realistic simulation of modification will follow improved treatments of cloud scale release of latent heat and the transfer of the released heat to the large scale. If these problems are solved, it is not too optimistic to expect models that will utilize observed initial data to make useful predictions of the behavior of individual storms by the end of the 1970's.

NOTATION

A available potential energy.
 c_p specific heat at constant pressure for dry air.
 $(d\theta/dt)_{L,S,R}$ material time rate of change of potential temperature due to latent heating (L), sensible heating (S), or infrared radiative cooling (R).
 E evaporation.
 f vertical component of earth's vorticity, approximately equal to $5 \times 10^{-5} \text{ s}^{-1}$ at 20°N .
 g acceleration of gravity.
 h Ekman depth, equal to $(2K_z/f)^{1/2} \sim 1 \text{ km}$.
 h_c height of cumulus cloud top above cloud base.
 H height of isobaric isothermal 'lid' on hurricane circulation.
 k specific kinetic energy, equal to $(u^2 + v^2)/2$.
 K total kinetic energy in hurricane domain.
 K_c vertical coefficient of kinematic (eddy) viscosity due to cumulus clouds.
 K_H horizontal coefficient of kinematic (eddy) viscosity.
 K_z vertical coefficient of kinematic (eddy) viscosity due to small-scale turbulence.
 l_h characteristic length scale for horizontal eddies.
 L latent heat of condensation.
 m relative angular momentum per unit mass, equal to rv .
 m_a absolute angular momentum per unit mass, equal to $rv + fr^2/2$.
 p pressure.
 p_r pressure on isentropic surface in hydrostatic barotropic reference atmosphere.
 P precipitation.
 P_c minimum pressure of hurricane.
 P_e pressure of 'undisturbed' hurricane environment.
 P_n normalized pressure.
 P_0 reference pressure, equal to 1000 mbar.
 q specific humidity.
 q_{sea} saturation specific humidity at sea surface temperature.
 \dot{Q} diabatic heating rate per unit mass.
 r radial distance from storm center.
 r_0 radius of hurricane domain, approximately equal to 1000 km.
 R gas constant for dry air.
 R_0 radius of maximum wind, approximately equal to 40 km.
 t time.
 T temperature.
 u radial wind component.
 u_c x component of momentum in cumulus clouds assumed to be equal to x component of momentum at cloud base.

u' horizontal eddy velocity.
 v tangential wind component.
 V wind speed.
 \mathbf{V} horizontal vector velocity.
 w vertical velocity.
 w_c vertical velocity in cumulus clouds.
 w_e vertical velocity of cumulus cloud environment.
 w' vertical eddy velocity.
 z height above sea level.
 $\langle \rangle_p$ average over pressure.
 $\langle \rangle_r$ average over radial distance.
 α percentage area covered by active cumulus convection.
 ζ_a absolute vorticity.
 θ potential temperature, equal to $T(P_0/p)^\kappa$.
 κ R/c_p .
 λ azimuth angle, positive counterclockwise.
 π total potential energy (sum of internal plus potential energy).
 π_r total potential energy of reference atmosphere.
 ρ density.
 σ area.
 τ_{zx} vertical shearing stress in x direction.
 τ_0 frictional stress at surface.
 ψ Montgomery potential, equal to $C_p T + gz$.
 ψ_r ψ of reference atmosphere.
 ω material time rate of change of pressure, vertical velocity in pressure coordinates.
 ∇ horizontal 'del' operator.
 ∇_θ del operator on isentropic surface.

Acknowledgments. The influence and guidance of Stanley L. Rosenthal, National Hurricane Research Laboratory, NOAA, over the years is gratefully acknowledged. He made many constructive criticisms of the original manuscript.

John A. Dutton made a very detailed review of an early version of the paper and provided many constructive suggestions. His effort is acknowledged with thanks.

Appreciation is also extended to Tanya Sharer, who carefully typed the manuscript.

Support for this research was provided in part by the National Science Foundation grant 1595 X to the Pennsylvania State University. Support was also provided by the Pennsylvania State University Computing Facility through the generous granting of computer time.

REFERENCES

- Anthes, R. A., The role of large-scale asymmetries and internal mixing in computing meridional circulations associated with the steady-state hurricane, *Mon. Weather Rev.*, 98(7), 521-528, 1970.
 Anthes, R. A., The response of a 3-level axisymmetric hurricane model to artificial redistribution of convective heat release, *NOAA Tech. Mem. ERL NHRL-92*, 14 pp., U.S. Dep. of Commer., Nat. Hurricane Res. Lab., Miami, Fla., 1971a.
 Anthes, R. A., A numerical model of the slowly varying tropical cyclone in isentropic coordinates, *Mon. Weather Rev.*, 99(8), 617-635, 1971b.
 Anthes, R. A., Numerical experiments with a slowly varying model of the tropical cyclone, *Mon. Weather Rev.*, 99(8), 636-643, 1971c.
 Anthes, R. A., The development of asymmetries in a three-dimensional numerical model of the tropical cyclone, *Mon. Weather Rev.*, 100(6), 461-476, 1972.
 Anthes, R. A., and D. R. Johnson, Generation of available potential energy in Hurricane Hilda (1964), *Mon. Weather Rev.*, 96(5), 291-302, 1968.
 Anthes, R. A., S. L. Rosenthal, and J. W. Trout, Preliminary results from an asymmetric model of the tropical cyclone, *Mon. Weather Rev.*, 99(10), 744-758, 1971a.
 Anthes, R. A., J. W. Trout, and S. L. Rosenthal, Comparisons of tropical cyclone simulations with and without the assumption of circular symmetry, *Mon. Weather Rev.*, 99(10), 759-766, 1971b.
 Arakawa, A., Parameterization of cumulus convection, *Proc.*

- WMO/IUGG Symp. Numer. Predict. Tokyo, 4(8), 1-6, 1969.
- Bjerknes, J., Saturated-adiabatic ascent of air through dry-adiabatically descending environment, *Quart. J. Roy. Meteorol. Soc.*, 64, 325-330, 1938.
- Black, P. G., and R. A. Anthes, On the asymmetric structure of the tropical cyclone outflow layer, *J. Atmos. Sci.*, 28(8), 1348-1366, 1971.
- Byers, H. R., *General Meteorology*, 540 pp., McGraw-Hill, New York, 1944.
- Carrier, G. F., A. L. Hammond, and O. D. George, A model of the mature hurricane, *J. Fluid Mech.*, 47, 145-170, 1971.
- Charney, J. G., and A. Eliassen, On the growth of the hurricane depression, *J. Atmos. Sci.*, 21(1), 68-75, 1964.
- Colon, J. A., et al., On the structure of Hurricane Daisy (1958), *Nat. Hurricane Res. Proj. Rep. 48*, 102 pp., Weather Bur. Office, Miami, Fla., 1961.
- Deacon, E. L., and E. K. Webb, Interchange of properties between sea and air, in *The Sea*, vol. 1, pp. 43-87, Interscience, New York, 1962.
- Deardorff, J. W., Numerical investigation of neutral and unstable planetary boundary layers, *J. Appl. Meteorol.*, 11(1), 91-115, 1972.
- Dunn, G. E., and B. I. Miller, *Atlantic Hurricanes*, 377 pp., Louisiana State University Press, Baton Rouge, 1964.
- Dutton, J. A., and D. R. Johnson, The theory of available potential energy and a variational approach to atmospheric energetics, *Advan. Geophys.*, 12, 333-436, 1967.
- Espy, J. P., *The Philosophy of Storms*, 552 pp., Little and Brown, Boston, 1841.
- Fletcher, R. D., Computation of maximum surface winds in hurricanes, *Bull. Amer. Meteorol. Soc.*, 36(6), 247-250, 1955.
- Garstang, M., Sensible and latent heat exchange in low-latitude synoptic scale systems, *Tellus*, 19(3), 492-508, 1967.
- Gentry, R. C., A study of hurricane rainbands, *Nat. Hurricane Res. Proj. Rep. 69*, 85 pp., U.S. Dep. of Commer., Weather Bur., Miami, Fla., 1964.
- Gentry, R. C., Project Stormfury, *Bull. Amer. Meteorol. Soc.*, 50(6), 404-409, 1969.
- Gentry, R. C., Hurricane Debbie modification experiments, August 1969, *Science*, 168(3930), 473-475, 1970.
- Gray, W. M., The mutual variation of wind, shear and baroclinicity in the cumulus convective atmosphere of the hurricane, *Mon. Weather Rev.*, 95(2), 55-73, 1967a.
- Gray, W. M., Global view of the origin of tropical disturbances and storms, *Atmos. Sci. Pap. 14*, 105 pp., Dep. of Atmos. Sci., Colo. State Univ., Fort Collins, 1967b.
- Gray, W. M., Cumulus convection and larger-scale circulations, 3, *Atmos. Sci. Pap. 190*, 80 pp., Dep. of Atmos. Sci., Colo. State Univ., Fort Collins, 1972.
- Haurwitz, B., The height of tropical cyclones and of the 'eye' of the storm, *Mon. Weather Rev.*, 63(2), 45-49, 1935.
- Hawkins, H. F., Vertical wind profiles in hurricanes, *Nat. Hurricane Res. Proj. Rep. 55*, 16 pp., Weather Bur. Office, Miami, Fla., 1962.
- Hawkins, H. F., and D. T. Rubsam, Hurricane Hilda, 1964, 2, Structure and budgets of the hurricane on October 1, 1964, *Mon. Weather Rev.*, 96(9), 617-636, 1968.
- Jacobs, W. C., Large scale aspects of energy transformations over the ocean, *Compendium of Meteorology*, pp. 1057-1070, American Meteorology Society, Boston, Mass., 1951.
- Johnson, D. R., The available potential energy of storms, *J. Atmos. Sci.*, 27(5), 727-741, 1970.
- Jordan, C. L., The thermal structure of the core of tropical cyclones, *Geophysica*, 6, 281-297, 1958.
- Jordan, C. L., Marked changes in the characteristics of the eye of intense typhoons between the deepening and filling stages, *Nat. Hurricane Proj. Rep. 44*, 20 pp., U.S. Dep. of Commer., Washington, D. C., 1961.
- Kuo, H. L., Dynamics of convective vortices and eye formation, in *The Atmosphere and the Sea in Motion*, pp. 413-424, Rockefeller Institute Press, New York, 1958.
- Kuo, H. L., On formation and intensification of tropical cyclones through latent heat release by cumulus convection, *J. Atmos. Sci.*, 22(1), 40-63, 1965.
- Lorenz, E., Available potential energy and the maintenance of the general circulation, *Tellus*, 7(2), 157-167, 1955.
- Machta, L., Evaporation rates based on tritium measurements for Hurricane Betsy, *Tellus*, 21(3), 404-408, 1969.
- Malkus, J. S., On the structure and maintenance of the mature hurricane eye, *J. Meteorol.*, 15, 337-349, 1958.
- Malkus, J. S., and H. Riehl, On the dynamics and energy transformations in steady-state hurricanes, *Tellus*, 12(1), 1-20, 1960.
- Malkus, J. S., and H. Riehl, *Cloud Structure and Disturbances Over the Tropical Pacific Ocean*, 229 pp., University of California Press, Berkeley, 1964.
- Malkus, J. S., C. Ronne, and M. Chaffee, Cloud patterns in Hurricane Daisy, *Tellus*, 13(1), 8-30, 1961.
- Margules, M., Über die Energie der Stürme, *Jahrb. Zentralanst. Meteorol.*, 1-26, 1903. (Translation by C. Abbe, *Smithson. Misc. Collect.*, 51, 553-595, 1910.)
- Meyers, V. A., On maximum hurricane winds, *Bull. Amer. Meteorol. Soc.*, 38(4), 1957.
- Miller, B. I., The three-dimensional wind structure around a tropical cyclone, *Nat. Hurricane Res. Proj. Rep. 15*, 41 pp., Weather Bur. Office, Miami, Fla., 1958.
- Miller, B. I., On the momentum and energy balance of Hurricane Helene (1958), *Nat. Hurricane Res. Proj. Rep. 53*, 19 pp., U.S. Dep. of Commer., Washington, D. C., 1962.
- Miller, B. I., A study of the filling of Hurricane Donna (1960) over land, *Mon. Weather Rev.*, 92(9), 389-406, 1964.
- Miller, B. I., Experiment in forecasting hurricane development with real data, *ESSA Tech. Mem. ERLTM-NHRL-85*, 28 pp., U.S. Dep. of Commer., Nat. Hurricane Res. Lab., Miami, Fla., 1969.
- Ogura, Y., Frictionally controlled, thermally driven circulations in a circular vortex with application to tropical cyclones, *J. Atmos. Sci.*, 21(6), 610-621, 1964.
- Ooyama, K., A dynamical model for the study of tropical cyclone development, *Geofis. Int.*, 4, 187-198, 1964.
- Ooyama, K., Numerical simulation of the life-cycle of tropical cyclones, *Contrib. 67*, 133 pp., Geophys. Sci. Lab., Dep. of Meteorol. and Oceanol., New York Univ., New York, 1967.
- Ooyama, K., Numerical simulation of the life-cycle of tropical cyclones, *J. Atmos. Sci.*, 26(1), 3-40, 1969.
- Ooyama, K., A theory on parameterization of cumulus convection, *J. Meteorol. Soc. Jap.*, 49, 744-756, 1971.
- Ostlund, H. G., Hurricane tritium 2: Air-sea exchange of water in Betsy 1965, *Proj. Rep. ML 67043*, 23 pp., Inst. of Mar. Sci., Univ. of Miami, Coral Gables, Fla., 1967.
- Palmén, E., On the formation and structure of tropical hurricanes, *Geophysica*, 3, 26-38, 1948.
- Palmén, E., and C. L. Jordan, Note on the release of kinetic energy in tropical cyclones, *Tellus*, 7(2), 186-189, 1955.
- Palmén, E., and H. Riehl, Budget of angular momentum and kinetic energy in tropical cyclones, *J. Meteorol.*, 14, 150-159, 1957.
- Pfeffer, R. L., Concerning the mechanics of hurricanes, *J. Meteorol.*, 15, 113-119, 1958.
- Riehl, H., *Tropical Meteorology*, 392 pp., McGraw-Hill, New York, 1954.
- Riehl, H., Some relations between wind and thermal structure of steady-state hurricanes, *J. Atmos. Sci.*, 20(4), 276-287, 1963.
- Riehl, H., and J. S. Malkus, Some aspects of Hurricane Daisy, 1958, *Tellus*, 13(2), 181-213, 1961.
- Riehl, H., T. C. Yeh, J. S. Malkus, and N. E. LaSeur, The northeast trade of the Pacific Ocean, *Quart. J. Roy. Meteorol. Soc.*, 77, 598-626, 1951.
- Rosenthal, S. L., Numerical experiments with a multilevel primitive equation model designed to simulate the development of tropical cyclones: Experiment 1, *ESSA Tech. Mem. ERLTM-NHRL-82*, 36 pp., U.S. Dep. of Commer., Nat. Hurricane Res. Lab., Miami, Fla., 1969.
- Rosenthal, S. L., Experiments with a numerical model of tropical cyclone development: Some effects of radial resolution, *Mon. Weather Rev.*, 98(2), 106-120, 1970a.
- Rosenthal, S. L., A circularly symmetric primitive equation model of tropical cyclone development containing an explicit water vapor cycle, *Mon. Weather Rev.*, 98(9), 643-663, 1970b.
- Rosenthal, S. L., A circularly symmetric primitive equation model of tropical cyclones and its response to artificial enhancement of the convective heating functions, *Mon. Weather Rev.*, 99(5), 414-426, 1971a.
- Rosenthal, S. L., The response of a tropical cyclone model to variations in boundary layer parameters, initial conditions, lateral boundary conditions, and domain size, *Mon. Weather Rev.*, 99(10), 767-777, 1971b.
- Rosenthal, S. L., An improved circularly symmetric model of the tropical cyclone, paper presented at Eighth Technical Conference on Hurricanes and Tropical Meteorology, Amer. Meteorol. Soc., Key Biscayne, Fla., May 14-17, 1973.

- Rosenthal, S. L., and M. S. Moss, Numerical experiments of relevance to Project Stormfury, *NOAA Tech. Mem. ERL NHRL-95*, 52 pp., U.S. Dep. of Commer., Nat. Hurricane Res. Lab., Coral Gables, Fla., 1971.
- Schauss, C. E., Reconstruction of the surface pressure and wind fields of Hurricane Helene, *Nat. Hurricane Res. Proj. Rep. 59*, 45 pp., U.S. Dep. of Commer., Washington, D. C., 1962.
- Shea, D. J., The structure and dynamics of the hurricane's inner core region, *Atmos. Sci. Pap. 182*, 134 pp., Dep. of Atmos. Sci., Colo. State Univ., Fort Collins, 1972.
- Sheets, R. C., On the structure of Hurricane Ella (1962), *ESSA Tech. Memo. IERTM-NHRL 77*, 36 pp., U.S. Dep. of Commer., Nat. Hurricane Res. Lab., Miami, Fla., 1967.
- Sheets, R. C., Some mean hurricane soundings, *J. Appl. Meteorol.*, 8(1), 134-146, 1969.
- Simpson, R. H., N. Frank, D. Shideler, and H. M. Johnson, Atlantic tropical disturbances, 1967, *Mon. Weather Rev.*, 96(4), 251-259, 1968.
- Sundqvist, H., Numerical simulation of the development of tropical cyclones with a ten-level model, 1, *Tellus*, 22(4), 359-390, 1970a.
- Sundqvist, H., Numerical simulation of the tropical cyclones with a ten-level model, 2, *Tellus*, 22(5), 504-510, 1970b.
- Sundqvist, H., Mean tropical storm behavior in experiments related to modification attempts, *Tellus*, 24(1), 6-12, 1972.
- Sverdrup, H. J., Evaporation from the oceans, *Compendium of Meteorology*, pp. 1071-1081, American Meteorology Society, Boston, Mass., 1951.
- Syono, S., A numerical experiment on the formation of tropical cyclones, *Proceedings International Symposium on Numerical Weather Prediction*, pp. 405-418, Meteorological Society of Japan, Tokyo, 1962.
- Yamasaki, M., A tropical cyclone model with parameterized vertical partition of released latent heat, *J. Meteorol. Soc. Jap.*, 46(3), 202-214, 1968a.
- Yamasaki, M., Detailed analysis of a tropical cyclone simulated with a 13-layer model, *Pap. Meteorol. Geophys.*, 19(4), 559-585, 1968b.
- Yanai, M., S. Esbensen, and J. Chu, Determination of bulk properties of tropical cloud clusters from large-scale heat and moisture budgets, *J. Atmos. Sci.*, 30(4), 611-627, 1973.

(Received November 20, 1973;
revised February 4, 1974.)